DOT/FAA/AND-97/1
DOT-VNTSC-FAA-97-1

Navigation and Landing
Product Team
Washington, DC 20591

United States Experience Using Forward Scattermeters For Runway Visual Range

David C. Burnham
Edward A. Spitzer
Thomas C. Carty
Deborah B. Lucas

U.S. Department of Transportation
Research and Special Programs Administration
John A. Volpe National Transportation Systems Center
Cambridge, MA 02142-1093

March 1997

This document is available to the public through the National Technical Information Service, Springfield, Virginia 22161

U.S. Department of Transportation
Federal Aviation Administration

REPORT DOCUMENTATION PAGE

Form Approved
OMB No. 0704-0188

1. AGENCY USE ONLY (Leave blank)	2. REPORT DATE	3. REPORT TYPE AND DATES COVERED
	March 1997	Final Report September 1996 - March 1997

4. TITLE AND SUBTITLE
United States Experience Using Forward Scattermeters for Runway Visual Range

5. FUNDING NUMBERS
FA795/A7090

6. AUTHOR(S)
D.C. Burnham,* E.A. Spitzer, T.C. Carty and D.B. Lucas

7. PERFORMING ORGANIZATION NAME(S) AND ADDRESS(ES)
Scientific and Engineering Solutions, Inc.*
16 Anchor Avenue
Orleans, MA 02653

8. PERFORMING ORGANIZATION REPORT NUMBER
DOT-VNTSC-FAA-97-1

9. SPONSORING/MONITORING AGENCY NAME(S) AND ADDRESS(ES)
U.S. Department of Transportation
Federal Aviation Administration
Navigation and Landing Products Teams
Washington, DC 20591

10. SPONSORING/MONITORING AGENCY REPORT NUMBER
DOT/FAA/AND-97/1

11. SUPPLEMENTARY NOTES
*under contract to:
U.S. Department of Transportation
Research and Special Programs Administration
John A. Volpe National Transportation Systems Center
Cambridge, MA 02142-1093

12a. DISTRIBUTION/AVAILABILITY STATEMENT
This document is available to the public through the National Technical Information Service, Springfield, VA 22161

12b. DISTRIBUTION CODE

13. ABSTRACT (Maximum 200 words)

The development of the forward scattermeter in the United States has spanned 25 years from the first design in 1969 to the 1994 commissioning of an airport runway visual range (RVR) system that uses a forward scattermeter rather than the conventional transmissometer to measure the atmospheric extinction coefficient. The forward scattermeter has many practical advantages over the transmissometer (single mounting pole, greater dynamic range, etc.). However, before a forward scattermeter could be accepted for an RVR system, a number of criteria had to be satisfied: (1) the calibration must be accurate and consistent (a) from one unit to the next and (b) for all important obstructions to vision (fog and snow for RVR); (2) the windows of the sensors must not clog in blowing snow; and (3) scatter measurements in a small volume of space must represent conditions over the runway as well as measurements made by a transmissometer which averages over a baseline (250 feet at US airports). Many different scattermeter designs were tested extensively, both in the field and in climatic chambers, before all acceptance criteria could be satisfied. The report describes the evolution of scattermeter design and presents the test methodology and results for the new RVR system.

14. SUBJECT TERMS
runway visual range, RVR, RVR system, visibility, extinction coefficient, forward scattermeter, forward-scatter visibility sensor, ambient light sensor, transmissometer

15. NUMBER OF PAGES
72

16. PRICE CODE

17. SECURITY CLASSIFICATION OF REPORT	18. SECURITY CLASSIFICATION OF THIS PAGE	19. SECURITY CLASSIFICATION OF ABSTRACT	20. LIMITATION OF ABSTRACT
Unclassified	Unclassified	Unclassified	

PREFACE

In 1969, the United States Air Force initiated the development of a forward scattermeter as an alternative to the conventional transmissometer for measuring the atmospheric extinction coefficient. After a decade and a half of further development, the Federal Aviation Administration (FAA) decided in 1985 to require the use of forward scattermeter technology in the Runway Visual Range (RVR) System Specification. In 1988, the FAA awarded a contract for a new generation RVR system which uses forward scattermeters. After a rigorous test program and two scattermeter redesigns, this system was declared ready for national deployment in August 1994.

This report documents the performance issues concerning the use of forward scattermeters and describes how they were addressed in the national deployment version of the new generation RVR system. As background information, the development history of the forward scattermeter is outlined.

This work has been conducted under the direction of three FAA RVR program managers: John Saledas, Calvin Miles and Deborah Lucas. The FAA's operational test and evaluation of the new generation RVR system has been directed by Tom Carty of the William J. Hughes Technical Center. The authors would like to acknowledge the support of many other colleagues over the last decade and a half, including:

Volpe Center: Charles Phillips, Mike West and Bob Pawlak

System Resources Corporation: Leo G. Jacobs, Clyde Lawrance, David Hazen and Bob D'Errico

Air Force Phillips Laboratory, Geophysics Directorate: Ralph Hoar, Gene Moroz, Leo P. Jacobs and Al Brown

Raytheon Service Corporation: John Crovo and Mike Jones

Teledyne Controls: Joel Liberty, Ghobad Karimi and Bill Gerhart

METRIC/ENGLISH CONVERSION FACTORS

ENGLISH TO METRIC

LENGTH (APPROXIMATE)

1 inch (in) = 2.5 centimeters (cm)
1 foot (ft) = 30 centimeters (cm)
1 yard (yd) = 0.9 meter (m)
1 mile (mi) = 1.6 kilometers (km)

AREA (APPROXIMATE)

1 square inch (sq in, in^2) = 6.5 square centimeters (cm^2)
1 square foot (sq ft, ft^2) = 0.09 square meter (m^2)
1 square yard (sq yd, yd^2) = 0.8 square meter (m^2)
1 square mile (sq mi, mi^2) = 2.6 square kilometers (km^2)
1 acre = 0.4 hectare (ha) = 4,000 square meters (m^2)

MASS - WEIGHT (APPROXIMATE)

1 ounce (oz) = 28 grams (gm)
1 pound (lb) = .45 kilogram (kg)
1 short ton = 2,000 pounds (lb) = 0.9 tonne (t)

VOLUME (APPROXIMATE)

1 teaspoon (tsp) = 5 milliliters (ml)
1 tablespoon (tbsp) = 15 milliliters (ml)
1 fluid ounce (fl oz) = 30 milliliters (ml)
1 cup (c) = 0.24 liter (l)
1 pint (pt) = 0.47 liter (l)
1 quart (qt) = 0.96 liter (l)
1 gallon (gal) = 3.8 liters (l)
1 cubic foot (cu ft, ft^3) = 0.03 cubic meter (m^3)
1 cubic yard (cu yd, yd^3) = 0.76 cubic meter (m^3)

TEMPERATURE (EXACT)

$°C=5/9(°F - 32)$

METRIC TO ENGLISH

LENGTH (APPROXIMATE)

1 millimeter (mm) = 0.04 inch (in)
1 centimeter (cm) = 0.4 inch (in)
1 meter (m) = 3.3 feet (ft)
1 meter (m) = 1.1 yards (yd)
1 kilometer (km) = 0.6 mile (mi)

AREA (APPROXIMATE)

1 square centimeter (cm^2) = 0.16 square inch (sq in, in^2)
1 square meter (m^2) = 1.2 square yards (sq yd, yd^2)
1 square kilometer (km^2) = 0.4 square mile (sq mi, mi^2)
10,000 square meters (m^2) = 1 hectare (ha) = 2.5 acres

MASS - WEIGHT (APPROXIMATE)

1 gram (gm) = 0.036 ounce (oz)
1 kilogram (kg) = 2.2 pounds (lb)
1 tonne (t) = 1,000 kilograms (kg) = 1.1 short tons

VOLUME (APPROXIMATE)

1 milliliter (ml) = 0.03 fluid ounce (fl oz)
1 liter (l) = 2.1 pints (pt)
1 liter (l) = 1.06 quarts (qt)
1 liter (l) = 0.26 gallon (gal)
1 cubic meter (m^3) = 36 cubic feet (cu ft, ft^3)
1 cubic meter (m^3) = 1.3 cubic yards (cu yd, yd^3)

TEMPERATURE (EXACT)

$°F=9/5(°C) + 32$

QUICK INCH-CENTIMETER LENGTH CONVERSION

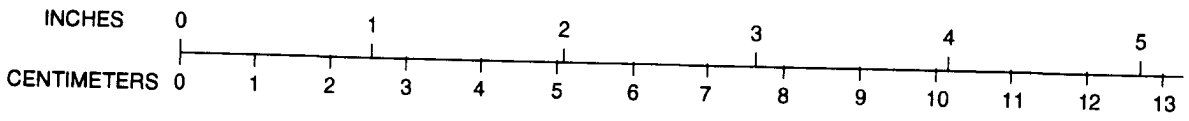

QUICK FAHRENHEIT-CELSIUS TEMPERATURE CONVERSION

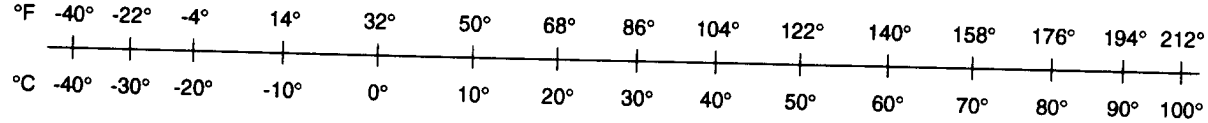

For more exact and or other conversion factors, see NIST Miscellaneous Publication 286, Units of Weights and Measures. Price $2.50. SD Catalog No. C13 10286.

Updated 8/1/96

TABLE OF CONTENTS

TABLE OF CONTENTS (cont.)

TABLE OF CONTENTS (cont.)

TABLE OF CONTENTS (cont.)

LIST OF FIGURES

LIST OF TABLES

1. INTRODUCTION

The purpose of this report is to document:

1. The rationale for adopting the forward scattermeter instead of the traditional transmissometer for the Federal Aviation Administration's (FAA) new generation runway visual range (RVR) system,
2. The problems encountered during the testing of this system and how they were resolved,
3. The observed performance of the forward scattermeter, and
4. Current activities designed to complete the validation of forward scattermeter technology.

This chapter provides background information on RVR and RVR systems. Chapter 2 describes the differences between transmissometers and forward scattermeters. Chapter 3 presents the critical issues for the acceptance of forward scattermeters for use in RVR systems. Chapter 4 outlines the historical development of the forward scattermeter in the United States. Chapter 5 describes the calibration process for the new FAA forward scattermeter. Chapter 6 addresses the performance of the new generation RVR system during precipitation. Chapter 7 describes ongoing work, and Chapter 8 presents the conclusions of the report.

1.1 SCIENCE OF VISION

The *visibility*, V, is defined as the greatest distance at which an object can be seen. The science of human vision has related visibility to the atmospheric extinction coefficient, σ, which can be measured automatically by an instrument. Standardized equations are used to estimate the visibility for black targets (Koschmieder's Law):

$$V = MOR = 3/\sigma \qquad (1)$$

and lights (Allard's Law):

$$E_T = I \exp(-\sigma V) / V^2 \qquad (2)$$

where I is the light intensity and E_T is the illumination detection threshold of the human eye. Note that Koschmieder's visibility is also termed meteorological optical range (MOR). Of course, these equations cannot account for non-ideal targets and variations from one observer to the next. Ideally, the extinction coefficient should be known over the entire distance between the target and the observer. In practice, a single instrument's measurement is used to represent the extinction coefficient over a considerable volume of space, extending both vertically and horizontally from the instrument's location.

1.2 RUNWAY VISUAL RANGE

Runway visual range (RVR) is an estimate of how far a pilot can see down a runway and is used to define operational limits on the use of precision instrument runways. RVR values are reported for

relatively low values of visibility, namely below 2000 meters or 6000 feet. At night, the only visibility targets are runway lights; therefore Allard's Law is used. In the daytime, either the runway lights or the runway markings may be more visible; to account for either possibility, the visibility of each is calculated using Allard's and Koschmieder's Laws and the greater value is reported as RVR.

RVR is used operationally to assess whether visibility conditions are good enough to allow a particular operation, such as an instrument landing. The highest RVR minimum is 800 meters for landing on a Category I runway. Thus, RVR measurements are operationally significant below 1000 meters or 3000 feet. For such low RVR values, runway lights set at maximum intensity will be more visible than runway markings. Consequently, whenever RVR is operationally important, Allard's Law is typically operative.

During the daytime, the pilot's illumination threshold, E_T, depends upon the background luminance level, B. Various equations have been assumed for this relationship; the new generation RVR system adopted the equation[1] (metric units):

$$\log (E_T) = 0.64 \log (B) - 5.7 \qquad (3)$$

1.3 AUTOMATED RVR SYSTEMS

An automated RVR system uses three sensors to estimate the RVR value:

1. Extinction coefficient (σ) sensor,

2. Background luminance (B) (or ambient light) sensor, and

3. Runway light intensity (I) monitor.

One-minute averages of extinction coefficient and background luminance are used to calculate RVR. Since the RVR estimate is most sensitive to extinction coefficient errors, more attention has been paid to the extinction coefficient than to the other two parameters. However, the other two parameters are subject to substantial uncontrolled variations that may result in comparable contributions to RVR errors[2].

The transmissometer is the traditional instrument for measuring extinction coefficient. Transmissometers designed for airport use were originally developed in the 1940s and 1950s. Since that era, developments in optics and electronics have been applied to improving transmissometer performance. However, the requirements for achieving and maintaining transmissometer accuracy are exacting and lead to costly installation and maintenance. In the late 1960s, development began on an alternative instrument, the forward scattermeter, which overcame most of the operational limitations of the transmissometer at the cost of a more complicated and less certain calibration method. In 1985, the FAA decided that forward scattermeter technology was mature enough to be considered in its RVR system specification. In 1988, a contract was awarded to Teledyne Controls for the manufacture of the FAA's new generation RVR system. Extensive field testing and two scattermeter redesigns led to deployment approval for this system in August 1994.

2. EXTINCTION COEFFICIENT INSTRUMENTS

This chapter first describes the characteristics of the atmosphere that are relevant to RVR and then describes principles of operation and characteristics of two instruments for measuring the atmospheric extinction coefficient: the transmissometer and the forward scattermeter.

2.1 OPTICAL CHARACTERISTICS OF THE ATMOSPHERE

For the purpose of the present discussion, the extinction coefficient must be separated into two components:

$$\sigma = \sigma_S + \sigma_A, \tag{4}$$

where σ_S is the scatter coefficient and σ_A is the absorption coefficient. The transmissometer responds to the total extinction coefficient σ while the forward scattermeter responds only to the scatter coefficient σ_S. RVR is concerned with visibility below 1500 meters. Fog is by far the most common obstruction to vision leading to such a low visibility. At many locations, snow is the next most common obstruction to vision leading to such a low visibility. For both snow and fog, the scatter coefficient is typically much larger than the absorption coefficient. Although rain is a common obstruction to vision, it rarely reduces the visibility below 1500 m unless it is accompanied by fog. Smoke, dust and sand are the three remaining obstructions to vision that can reduce the visibility below 1500 m; although they are rare in most United States (US) locations, they can be expected to have significant absorption.

2.2 TRANSMISSOMETER

2.2.1 Operating Principle

The attenuation of light passing through the atmosphere is given by the equation:

$$I = I_0 \exp(-\sigma b), \tag{5}$$

where I_0 is the intensity with no obstruction to vision, I is the intensity with an obstruction to vision having an extinction coefficient σ and b is the distance between the light source and the observation point.

The transmissometer is an instrument based on Equation 5. A projector transmits a light beam toward a receiver located a distance b away. The receiver measures the intensity I of the beam after it has passed through the atmosphere. The transmissometer measurement equation is given by a nonlinear relationship, obtained by rearranging Equation 5:

$$\sigma = -(1/b) \ln(I/I_0). \tag{6}$$

Equations 5 and 6 assume that, once light has scattered out of the beam, it will not experience additional scattering that will put it back into the beam (i.e., no multiple scattering). Multiple scattering can, therefore, lead to errors in transmissometer measurements. The projector beam divergence and receiver field of view must be kept small to avoid significant multiple-scatter errors.

2.2.2 Calibration

The calibration of the transmissometer depends upon knowing the clear air intensity I_0. If the true value of I_0 is equal to the assumed value times a factor f, the extinction coefficient error is given by a fixed offset:

$$\Delta\sigma = (1/b)\ln(f). \qquad (7)$$

This offset error limits the ability of a transmissometer to measure low extinction coefficients (i.e., high values of visibility). The other source of error in a transmissometer is a measurement error ΔI in the intensity I. The resulting error in extinction coefficient is given by:

$$\Delta\sigma/\sigma = (1/b)\ln(1+\Delta I/I). \qquad (8)$$

This error becomes large when the extinction coefficient is large (i.e., low values of RVR). The net effect of the errors in Equations 7 and 8 is that a transmissometer can measure accurately only over a band of σ values. The valid MOR values (Equation 1) typically range from 2/3 of the baseline to twenty times the baseline; thus, the dynamic range is about a factor of 30. Very careful attention to calibration accuracy and stability and photodetector dynamic range is needed to extend these limits significantly. Most transmissometer systems use two baselines to cover the full RVR range (MOR from 10 to 1500 meters, factor of 150).

In practice, transmissometers at airports are calibrated on clear days. After cleaning the transmitter and receiver optics, the technician estimates the visibility and sets the transmissometer to the appropriate transmission value. This process is somewhat hit or miss since times of calibration are random and affected by the estimates of visibility.

If the transmissometer windows are well protected against contamination, automated calibration is possible by assuming that the contamination builds up at a small constant rate (percent loss per day). The assumed contamination loss is used to correct the clear-air intensity value I_0. If the assumed rate of contamination buildup is greater than the actual rate, then the transmission will become higher than 100 percent on a clear day and the assumed value of I_0 can be reset to the actual value. This procedure will keep the transmissometer reasonably accurate if the contamination corrections are small and clear days occur regularly (e.g., every 3 or 4 days).

2.2.3 Advantages/Disadvantages

As mentioned in Section 2.2.1, the assumption of single scattering that governs Equation 5 places severe restrictions on the design of transmissometers[3]. In order to prevent multiple scattering from influencing the measurement, the transmissometer projector beam and receiver field of view must be kept very narrow. The narrow beams necessitate rigid mounting towers so that the beam alignment remains stable. The narrow beam requirement also means that it is not practical to use the same optical units for a short baseline transmissometer as for a long baseline transmissometer. For example, the Unites States transmissometer-based RVR system was originally designed to cover the full RVR range using a common projector and two separate receivers on baselines of 12 and 76 meters. Tests[4] at

the Atlanta, GA airport showed (1) alignment problems, and (2) a multiple-scatter error of about 20 percent for the short baseline (measured extinction coefficient too low).

The primary advantages of the transmissometer over the scattermeter are:

1. The extinction coefficient is determined directly from Equation 6 with no assumptions, and

2. Each transmissometer can be calibrated by itself (on a clear day) with no external references.

In general, these advantages should result in a transmissometer giving a more accurate extinction coefficient measurement than a scattermeter. It should be noted, however, that a transmissometer is more accurate than a scattermeter only if it is well maintained.

The considerable efforts to develop the scattermeter as a transmissometer replacement are due to the following costs and problems associated with the transmissometer; many are related to installation and maintenance:

1. Frost heaves or other soil instabilities can throw the projector and receiver out of alignment.

2. Measurements are very sensitive to window contamination (Equation 7). Window cleaning may be required weekly.

3. It is difficult to design a transmissometer tower that is both rigid and frangible. A transmissometer tower is, therefore, a potential collision hazard to an aircraft.

4. Either two baselines or a very sophisticated design are needed to cover the full RVR range.

5. High visibility conditions are needed to recalibrate a transmissometer after a maintenance action.

6. The US transmissometer (see next section) also suffers from sensitivity to sunlight. Such sensitivity has been eliminated in other countries by modulating the light source.

2.2.4 US Transmissometer

The current US transmissometer is shown in Figure 1; the rigid mounting towers are used to preserve beam alignment. The

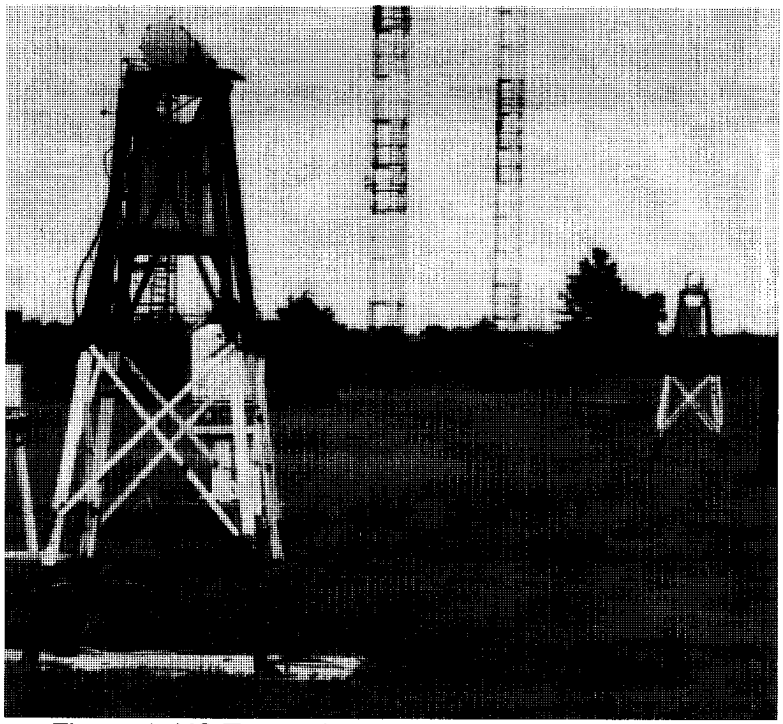

Figure 1. US Transmissometer at Otis Weather Test Facility: View from Receiver toward Projector

transmissometer design has changed little since its first development in the late 1940s. Only the electronics have been upgraded. For example, a silicon photodiode has replaced the original vacuum photodiode. The 22-cm diameter incandescent projector lamp contains an internal parabolic reflector. Since the light is not chopped, the receiver is sensitive to sunlight. The lamp is turned off every hour to measure the background sunlight. The background light measurement is then subtracted from the light measurement for the next hour. Since no wavelength-dependent filter is installed in the transmissometer, much of the instrument's response comes from red and infrared light (with wavelengths as high as 1.1 microns, the cutoff wavelength for silicon photodiodes). Therefore, the measurements may not represent human vision, which responds to wavelengths of 0.4 to 0.8 microns, with peak response at 0.55 microns. Section 5.2.2.2 discusses the small effect of this infrared response on the measurement of the fog extinction coefficient, which is almost independent of wavelength.

2.3 SCATTERMETER

2.3.1 Operating Principle

In contrast to the transmissometer that measures the attenuation of a light beam, a scattermeter directly measures the light scattered out of a small portion of a light beam. If all the scattered light could be collected, the scattered signal would be proportional to the scatter coefficient. Instruments intended to collect all the scattered light have not been very successful, however, because the receiver interferes with the free flow of the scattering particles through the scatter volume. A scattermeter gets around the obstruction problem by moving the transmitter and receiver away from the scatter volume and by making them small. As a result, a scattermeter collects scattered light over only a small range of scattering angles. Such a measurement can make a valid estimate of the extinction coefficient if two assumptions are satisfied:

1. The absorption coefficient is assumed to be much smaller than the scatter coefficient. Therefore an estimate of the scatter coefficient (Equation 1) is a valid estimate of the extinction coefficient:

$$\sigma_S \approx \sigma \tag{9}$$

   As will become obvious in the Section 2.3.2 discussion of scattermeter calibration, the actual assumption is somewhat less stringent. The scattermeter calibration will also be correct if the absorption coefficient is proportional to the scatter coefficient so that the scatter coefficient is proportional to the extinction coefficient:

$$\sigma_S \propto \sigma. \tag{10}$$

2. The scattering S measured by the scattermeter is assumed to be proportional to the scatter coefficient.

$$S \propto \sigma_S \tag{11}$$

   The scattermeter receiver collects light scattered from the transmitter beam over a range of scattering angles that is defined by the geometry of the unit. If all obstructions to vision scatter light in a similar fashion, this assumption would be easy to justify. Unfortunately, significant

differences in scattering characteristics exist for different obstructions to vision (e.g., fog and snow for RVR) or even different forms of the same obstruction to vision. However, the selection of an appropriate range of angles may give approximate proportionality of the scattered signal to the scatter coefficient for most common conditions.

The use of forward scattering angles in the range of 25 to 50 degrees was found to give scattering in fog that was approximately proportional to the scatter coefficient and more or less independent of the drop-size distribution of the fog. In the development of the US RVR forward scattermeter, described in Section 4.5.1.2, it was found that using a nominal scattering angle of 42 degrees gives approximately equal calibration in fog and snow.

2.3.2 Calibration Method

The calibration equation for a forward scattermeter is (see Equations 10 and 11):

$$\sigma = K\,S. \qquad (12)$$

Note that no σ offset has been included in the calibration equation. A well designed scattermeter has little electronic (Section 4.1) or optical (Section 4.2.1) offset. The calibration constant K depends upon a host of parameters, including:

1. Transmitter light intensity,
2. Receiver gain,
3. Transmitter beam geometry,
4. Receiver beam geometry, and
5. Average scattering angle.

Since many of these parameters are not completely defined, there is no way of calculating the absolute calibration of a forward scattermeter. The only practical calibration method is to compare the scattermeter measurements to concurrent transmissometer measurements. Section 5.2 describes one method for making this comparison. The following two sections explain how the calibration process is implemented.

2.3.2.1 Scatter Plate Calibrator

The many variables affecting a scattermeter's calibration pose a problem for setting and maintaining sensor calibration. The solution to this problem is to build a calibrator that generates a standardized amount of scattering. The calibrator consists of a diffuse scattering plate combined with an attenuator to reduce the scattered signal into the dynamic range of the sensor. The plate and attenuator may be separate units or combined into a single unit.

Note that the signal attenuation is typically a factor of 100 to produce a fog equivalent extinction coefficient of 100 km^{-1}. Therefore, if a sensor is calibrated in dense fog having the same extinction

coefficient of 100 km^{-1}, the additional scattering from the fog will give a calibration error of only one percent. Thus, calibration of a forward scattermeter in dense fog will give little calibration error.

2.3.2.2 Calibration Transfer

While conventional transmissometers can be calibrated directly in the field (on a clear day), the calibration of a forward scattermeter must be referenced to transmissometer measurements. The reference transfer method involves at least three steps:

1. A number of forward scattermeter units are operated at a location with reference transmissometers to determine their response to fog, the most common obstruction to vision for RVR. The scattermeter gain is adjusted to agree with the transmissometers.

2. Scatter-plate calibrators, which simulate the scattering from fog, are then measured in the calibrated forward scattermeter units and marked with their measured extinction coefficient.

3. A measured scatter-plate calibrator is then installed in an airport forward scattermeter and the sensor gain is adjusted to give the reading marked on the calibrator.

This calibration procedure eliminates most of the instrumental errors from the measurements of a forward scattermeter.

2.3.2.3 Calibration Consistency

The forward scattermeter calibration method assumes that scattering from a diffuse plate is proportional to the volume scattering from fog. The ratio of plate scattering to volume scattering will be constant only if the scattering geometry is identical for each scattermeter unit. In other words, the manufacturing tolerances will determine the unit-to-unit variation of the forward scattermeter calibration.

2.3.3 Advantages/Disadvantages

A forward scattermeter has many practical advantages over a transmissometer:

1. It is much less sensitive to window contamination.

2. It can be mounted on a single frangible pole.

3. A single unit can cover the full RVR measurement range.

4. It can be recalibrated under most poor visibility conditions.

The disadvantages of the scattermeter over the transmissometer are primarily related to calibration, although other questions can be important:

1. A scattermeter cannot be calibrated by itself. Its calibration must be traced to a transmissometer.

2. Its calibration may depend upon the obstruction to vision, both because of scattering variations for a given obstruction to vision such as fog and for different obstructions to vision, such as snow and dust.

3. Its calibration may vary from one unit to the next.

4. Snow clogging of a scattermeter leads to unconservative (i.e., higher) values of RVR in contrast to snow clogging of transmissometer which leads to conservative (i.e., lower) values of RVR.

5. The small measurement volume of a scattermeter may give a less representative value of the extinction coefficient than the transmissometer which averages over its baseline.

2.3.4 US RVR Scattermeter

Figure 2 shows the final scattermeter design for the FAA's new generation RVR system. Its overall size is about one meter and it is mounted on a frangible fiberglass pole. It features a "look-down" geometry to minimize window contamination, removable hoods for window cleaning, removable heads for service convenience and bird spikes to discourage birds from perching on the hoods and blocking the beams. The heads are angled out of the plane of the yoke so that the beams will not intersect the mounting arms. Section 4.5.1 presents more details about its design and operation.

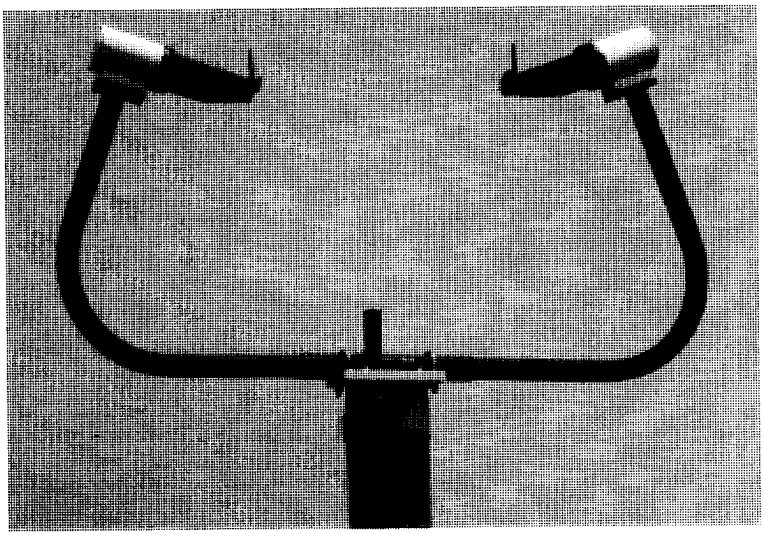

Figure 2. National Deployment Forward Scattermeter

3. FORWARD SCATTERMETER ACCEPTANCE ISSUES

Although forward scattermeters have many advantages over transmissometers, they are not superior in all respects. Five performance issues have been raised as critical to forward scattermeter acceptance. The first four are specific to the scattermeter design and are therefore addressed in Chapters 5 and 6 for the new generation RVR system. The fifth is generic to all scattermeters and is therefore discussed only in this chapter.

3.1 CALIBRATION VARIATION

3.1.1 Different Fogs

Fog is the most common obstruction to vision leading to significant values of RVR. Fogs are characterized by their drop-size distribution and by the nature of the nuclei on which the drops condense, which may affect the absorptive properties of the droplets. Since the angular scattering function can vary significantly for different drop sizes, in principle, different drop-size distributions could give significant differences in fog calibration (Equation 12).

The physics of scattering from water droplets is relatively straight forward. The scattering consists of two equal components:

1. The direct scattering of light that hits the droplet, and

2. The diffraction scattering of the hole left in the incident light beam.

When the particle is much larger than the wavelength of light, the direct scattering is similar for all particle sizes, but the diffraction scattering is concentrated in the forward direction with an angle spread proportional to the ratio of the wavelength of light to the particle diameter. Thus, for large droplets, where the diffraction scattering is at smaller angles than those measured by a forward scattermeter, the scattered signal will be produced only by direct scattering and will be approximately proportional to the extinction coefficient for any size droplet above a certain size limit. The predominant droplet diameter in fog is typically 5 microns or greater, which is much larger than the wavelength (0.9 microns or smaller) used by forward scattermeters. Hence, one would expect that the fraction of scattered light detected by a forward scattermeter would be similar for all types of fog and the fog calibration should not depend much upon the drop-size distribution.

However, for smaller droplets, e.g., those characteristic of haze, some diffraction scattering will be detected at the forward scattermeter angle. Consequently, the response of the scattermeter (Equation 11) to haze of a given scatter coefficient is higher (typically 40 percent higher for the same wavelength) than the response to fog with the same scatter coefficient.

Although theoretical considerations suggest that a forward scattermeter will have a reasonably consistent response to fogs with different drop-size distributions, experimental data are needed to validate the fog calibration consistency for real instruments measuring real fogs. Data on the variation of the fog calibration for the US RVR forward scattermeter are presented in Section 5.3.2. [Note that drop-size distributions were not measured.] Section 5.3.2.2 presents the spread in scattermeter-

transmissometer measurement ratio. Typically half the measurements agree to within ± 5%. Section 5.3.2.3 discusses the variation in scattermeter-transmissometer measurement ratio with wind direction. Disaggregating the data by wind direction appears to isolate fogs with different scattering characteristics. The observed angular variation in median scattermeter-transmissometer measurement ratio was at most ±7%.

3.1.2 Unit to Unit

Fog calibration variations from one scattermeter unit to the next have been noted in many tests, most notably the 1988-89 World Meteorological Organization (WMO) test[5]. The cause for the observed calibration variations was first identified in 1986 tests conducted at the Seattle-Tacoma Airport. One of three forward nominally identical scattermeter units, calibrated with the same calibrator, was observed to have a significantly different fog calibration than the other two. Analysis of the three units showed that the transmitter beam divergence angle was greater for that unit than for the other two. Thus, the unit-to-unit calibration consistency was found to depend upon the manufacturing tolerances for defining the scattering geometry.

As discussed in Section 2.3.2.3, scattermeter calibration consistency depends upon keeping a constant ratio between the plate scattering from the calibrator and the volume scattering from fog. A calibration simulation computer model was developed (Section 5.1) to calculate how this ratio varies for different manufacturing errors. The model was first used to design scattering geometries for the US RVR forward scattermeter that are insensitive to manufacturing errors (Section 5.1.1). The model was then adapted (Section 5.1.3) to use precision measurements of US RVR scattermeter yoke geometry to assess the expected distribution of calibrations (maximum of about ±5% variation from yoke errors). The best field measurements presented in Section 5.3.3.1 show a unit-to-unit fog calibration variation of ±1.5% for units that were selected to have close to nominal measured scattering geometry.

3.1.3 Different Obstructions to Vision

Section 3.1.1 considered how the calibration of a forward scattermeter could vary for fogs with different scattering characteristics. Although fog is the most common obstruction to vision reducing the visibility into the RVR region, other obstructions to vision, such as snow, smoke, dust, or sand, can also lead to such low visibilities. Note that smoke, dust and sand may have significant absorption, which may result in measurement errors (see Section 2.1).

In the US, snow is the next most frequent RVR obstruction to vision after fog and has therefore received careful consideration in the development of the US RVR forward scattermeter. The final scattering angle was selected to give approximately equal fog and snow calibrations. Section 5.3.3 presents experimental data on the relative calibration in fog and snow.

3.2 SNOW CLOGGING

All optical sensors operating in the outdoor environment are subject to clogging by blowing snow. This problem is more tolerable for transmissometers than scattermeters because of the operational implications of the clogging. A clogged transmissometer will report a conservative (i.e., lower) RVR value rather than the actual value. A lower RVR value may force the closing of a runway that should

be operable, but will not mislead a pilot into expecting to see the runway when he cannot. On the other hand, a snow-clogged scattermeter will typically lead to non-conservative (i.e., higher) values of RVR.

The development of the US RVR forward scattermeter was largely successful in eliminating snow clogging by adopting a look-down scattering geometry and by suitable design and heating of the sensor's protective hoods and windows. Section 6.2 describes the tests that addressed snow clogging of the forward scattermeter and the ambient light sensor. Although the reported RVR value is much less sensitive to ambient light reading than extinction coefficient, snow clogging turns out to be more serious for the ambient light sensor which cannot use a look-down geometry because it must view the sky.

3.3 SPATIAL REPRESENTATIVENESS

Although an extinction coefficient sensor measures at a specific spatial location, the measurement is used to represent the extinction coefficient over a volume of space. For example, US installation procedures permit a single sensor to provide RVR data for locations within 600 meters of the sensor.

The representativeness of a measurement can, in principle, be improved by averaging over a larger volume of space; such averaging will reduce the influence of small-scale fluctuations on the measurement. Thus, one might expect that a forward scattermeter, which averages over a volume of about 0.03 cubic meters, could be less representative than a transmissometer, which averages along its baseline (76 meters in the US, but only 10 meters in the UK). The significance of this difference in measurement volume will be examined from three points of view:

1. The effect of wind on the measurement,
2. The ratio of the measurement volume to the distances over which the measurement is used, and
3. A direct assessment of representativeness using instrument comparisons from the Otis Weather Test Facility (WTF) and the Seattle-Tacoma Airport.

3.3.1 Wind Averaging Effect

RVR is calculated from a one-minute average of the extinction coefficient (Section 1.3). If the wind blows at 1.2 m/s, approximately 75 meters of the atmosphere will pass through the scatter volume of a forward-scatter sensor in the 60-second averaging time. Thus, one would expect that the spatial averaging of a forward-scatter sensor will be approximately as good as that of a transmissometer whenever the wind speed is greater than 1.2 m/s.

3.3.2 Relative Averaging Volume

When the wind is less than 1.2 m/s, such as occurs during radiation fog, the greater spatial average of the transmissometer may provide a somewhat better estimate of the extinction coefficient. However, it should be noted that the US transmissometer is located at twice its averaging distance (150 meters) away from the runway. Moreover, the distance it is supposed to represent (600 meters) is eight times the averaging distance. When the fog is patchy, the fog density can vary dramatically over 150 meters,

not to mention 600 meters, and the 76-meter average will likely not provide much improvement over the "point" measurement of the forward-scatter sensor. Neither will provide a very representative measurement under such conditions.

3.3.3 Direct Assessment

Since wind speed and fog patchiness affect the relative representativeness of the transmissometer and the forward-scatter sensor in complicated ways that cannot be readily modeled, it is useful to examine airport data to assess the representativeness of sensor visibility measurements.

The methodology is to use one sensor, preferably a transmissometer, as the reference for the "actual" extinction coefficient and compare the measurements from a transmissometer and a scattermeter that are displaced from the location of the reference sensor. The analysis was performed on data from the Otis WTF (Section 5.2.1), which provides data on the minimum displacement (150 meters) between the sensor and the location to be represented, and the Seattle-Tacoma Airport, which provides data on the maximum displacement (600 meters) to be represented.

3.3.4 Otis Comparisons

The methodology used for the Otis comparisons is described in Appendix A. The Otis site permits a comparison between two 152-meter-baseline transmissometers that are displaced by 152 meters, which is just the displacement of a US extinction coefficient sensor from the runway centerline. The representativeness of a measurement is indicated by the width of the FOG box in a box plot (see Figure 16); a smaller box width means better representativeness. The position of a transmissometer is taken as the midpoint of its baseline. Results were obtained for two different displacements between the sensors and the reference transmissometer:

Displacement	Results
0 m	Box width for transmissometer roughly half that observed for forward scattermeters. Thus, transmissometer significantly more representative than scattermeter.
152 m	Box width increases for both types of sensors and becomes comparable.

Since the 152-meter displacement corresponds to the minimum US separation between the extinction coefficient sensor and the strip of runway it is required to represent, one can conclude that there is no significant difference in the operational representativeness of the transmissometer and the forward scattermeter.

3.3.4.1 Sea-Tac Comparisons

The initial installation of the new generation RVR system at the Seattle-Tacoma Airport (Sea-Tac) provided an opportunity to examine representativeness at the US 600-meter upper distance limit on representativeness. The transmissometers at Sea-Tac were located in the conventional touchdown, midpoint and rollout positions. The new generation touchdown and midpoint sensors were located near the corresponding transmissometers. Because of runway expansion plans, the new generation "rollout" sensor was installed roughly midway between the midpoint and rollout transmissometers. Thus, it was located roughly 600 meters away from the midpoint new generation sensor and the midpoint and rollout transmissometers. In particular, it can serve as a test of how well the two

midpoint sensors can represent the extinction coefficient approximately 600-meters away. Similarly, the touchdown and rollout sensors can show how well the two midpoint sensors can represent the extinction coefficient approximately 1200 meters away.

The Sea-Tac analysis was complicated and will not be presented here. The results from the period 11/4/91 - 4/13/92 generally showed comparable representativeness for the transmissometers and forward scattermeters and were used to satisfy US authorities that the installation representativeness limit of 600 meters need not be reduced for the new generation RVR system.

4. US FORWARD SCATTERMETER DEVELOPMENT HISTORY

This chapter outlines the development history of the forward scattermeter in the United States. Although some work has been done in other countries, only information about US-manufactured sensors will be presented here. The features needed for a robust sensor were discovered slowly over the course of one and a half decades of development. The developments of optical technology will be followed by a discussion of the advantages and disadvantages of different scattering geometries.

4.1 TECHNOLOGY

The primary technological issues for forward scattermeters are the type of light source and the method of modulation. Modulating the light source and synchronously detecting the received signal can make the instrument insensitive to ambient sunlight. Since the scattered signals are very small, proper design practices must be followed to isolate the receiver electrically from the transmitter and thereby prevent electronic offsets.

4.1.1 Light Choppers

The first forward scattermeter[6], developed by the US Air Force, used a mechanically chopped incandescent light source, with a chopping frequency of 300 Hz. Since the sensor field of view (see Figure 3) included the horizon and the ground, this sensor occasionally suffered from "glint" problems where sunlight scattered from an object (perhaps shaking in the wind) within its field of view generated signals within the operating bandwidth of the sensor. Both incandescent lamps and mechanical choppers are high maintenance items.

4.1.2 Modulated Light Emitting Diodes

The introduction of electrically modulated light emitting diodes (LED) dramatically increased the reliability of the scattermeter. The modulation frequency was raised to the 2-4 kHz region where sunlight interference was much less a problem. The diodes last for many years with relatively little loss in intensity; photodetector feedback controls the LED drive current to keep the intensity steady. Infrared emitting diodes are normally used in scattermeters because they are more intense and more reliable than visible light diodes. The spectrum of the emission is typically centered at about 0.9 microns wavelength; most scattermeters use a narrow band optical filter in the receiver to reject sunlight outside the emission band. As discussed in Section 3.1.1, the use of infrared light affects scattermeter performance for small scattering particles[7] (e.g., haze) and high visibilities. However, infrared light should normally give accurate RVR estimates because the more operationally significant obstructions to vision (fog and snow) have little variation of scattering with wavelength (dense smoke could be an exception).

4.1.3 Flashlamps

The flashlamp is the final light source used in forward scattermeters. Because the light is very bright and concentrated into a time of a few microseconds, the signal-to-noise ratio is higher for a scattermeter using a flashlamp than for units using other light sources. The light spectrum from a flashlamp is actually shifted toward the blue compared to the human visual response. This difference

may affect the response to small scattering particles (in the opposite direction from that observed for infrared LEDs), but has little impact on RVR performance.

4.2 GEOMETRY

The geometry of a forward scattermeter has many different effects on sensor performance. The geometry encompasses:

1. Transmitter and receiver beam shapes and their overlap to form the scattering volume,
2. Baffles and hoods used to protect the sensor windows and to prevent transmitted light from reaching the receiver via surface scattering,
3. The structures used to support the heads, and
4. The location of the electronic control box.

4.2.1 Multiple Surface Scattering

The signal produced by scattering from aerosols is very small when the visibility is high. Multiple scattering from solid objects can easily generate comparable sized signals unless the sensor geometry is carefully designed. Such scattering will result in a zero signal shift or "offset," which would need to be subtracted from the total scattered signal S in Equation 12 to give a correct measurement of extinction coefficient. Since no scattering objects are located in the sensor scatter volume, scattering offsets most easily result from double scattering, i.e., from an object illuminated by the transmitter to an object viewed by the receiver.

The scattering objects leading to calibration offsets can be the sensor hood, dirt on the sensor window, the sensor mount or even the ground. For example, the transmitter and receiver windows must be baffled so that they cannot see each other; otherwise, dirt on the two windows will provide an efficient double-scatter route for transmitted light to reach the receiver. A suitable hood around the sensor windows can prevent the windows from seeing each other. However, the transmitter and receiver beams must not hit the hood; otherwise, double hood scattering will again produce undesirable surface scattered signals. The transmitter and receiver beams should also not hit the sensor mounts. Making all surfaces black to the operating light spectrum will also reduce multiple scattering. Experience has shown that scattering from the ground is not a problem if these design criteria are followed.

4.2.2 Scatter Volume

The size of the scattering volume can affect the variance of the extinction coefficient measurement. This effect is particularly important in precipitation where the number of particles, N, passing through the scatter volume during one averaging time can determine the standard deviation of the measurement:

$$\Delta\sigma/\sigma \approx N^{-1/2}, \qquad (13)$$

Fog also has microstructure that can affect the variance of the measurement if the scatter volume is too small.

The design of a forward scattermeter involves tradeoffs between sensor size and signal-to-noise ratio:

1. The scatter volume is proportional to the cube of the spacing between the transmitter and receiver heads. The scatter volume provides averaging over fog microstructure.
2. The projected area of the scatter volume is proportional to the square of the head spacing. This area provides averaging over precipitation particles.
3. The signal-to-noise ratio of a scattermeter is inversely proportional to the head spacing.

To illustrate these tradeoffs, a factor of two decrease in signal-to-noise ratio can be traded for a factor of eight increase in volume and a factor of four in projected area. However, the price of this trade is doubling the size of the scattermeter, which could make it less practical. Similar increases in volume/area can be achieved by doubling the beam width; however, this option may lead to problems in setting the desired scatter angle or protecting the sensor windows from snow or scattered light.

4.2.3 Wind Shadowing

The size and positioning of the sensor heads and mounts relative to the scatter volume can significantly affect the scattermeter performance. The heads and/or mounts can collect or block fog and snow particles so that the particle density in the scatter volume is not representative of the atmosphere as a whole. In this case, the sensor response may depend upon the wind direction. This effect is minimized if heads and mounts are small and as far away as possible from the scatter volume.

4.2.4 Heating Effects

Fog density is very sensitive to air temperature. Heat generated by the sensor, e.g., hood heaters, may increase the air temperature and hence reduce the fog density. Heating effects can be minimized by keeping heat sources above or far away from the scatter volume.

4.2.5 Annular Beams

Figure 3 shows the first[6] forward scattermeter. Both transmitter and receiver beams were annular; the scatter region where the two beams overlap is doughnut shaped. This scattering geometry maximizes the scatter volume for a given size sensor. However, the divergence of the beam in all directions makes it difficult to design a hood to protect the sensor from snow clogging. Most later sensor designs adopted simpler beam shapes.

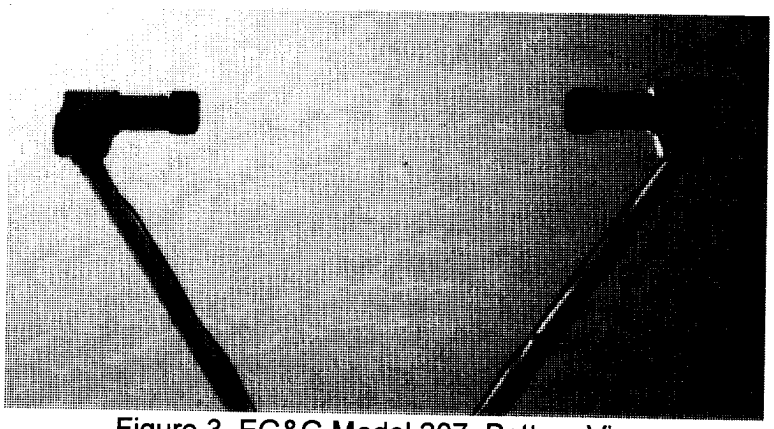

Figure 3. EG&G Model 207, Bottom View

Note that, even though this was the first forward scattermeter, care was taken to keep the heads and mounts small to minimize their effects on the measurement. The sensor arms were attached directly to the electronics box, but were oriented diagonally so that heat rising from the electronics would not affect the fog in the scatter volume under no-wind conditions. The engineering tradeoffs needed to pack the light chopper into a small space led to enough maintenance problems that these units are no longer in service.

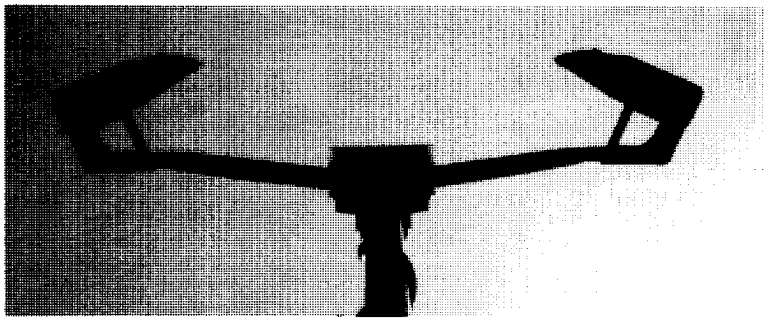

Figure 4. HSS VR-301B, Bottom View

4.2.6 Horizontal Beams

Horizontal beams were used for most of the United States forward scattermeters developed during the 1980s. Figure 4 shows the latest version of the first modulated LED forward scattermeter. The first version had much shorter mounting arms and suffered from wind shadowing effects. This sensor was the inspiration for the two additional sensors shown in Figures 7 and 8.

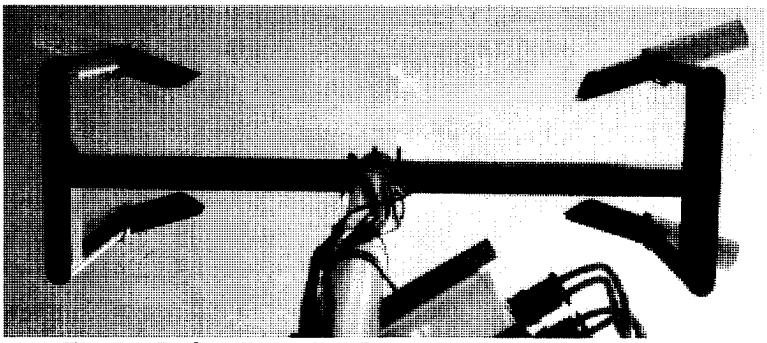

Figure 5. Qualimetrics Scattermeter, Bottom View

Figure 5 shows the Qualimetrics forward scattermeter, which is used in the FAA's Automatic Weather Observing System (AWOS) and the new Canadian RVR system. It uses four heads, two transmitters and two receivers, to correct for window contamination (see Section 4.2.8).

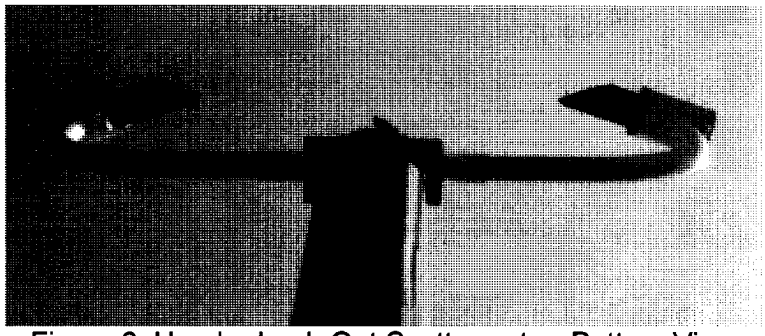

Figure 6. Handar Look-Out Scattermeter, Bottom View

Figure 6 shows the original design of the Handar forward scattermeter, which was adopted for the FAA's new generation RVR system; Figure 7 shows a side view. The Handar scattermeter features removable heads, which facilitated the development of the final look-down version shown in Figure 2.

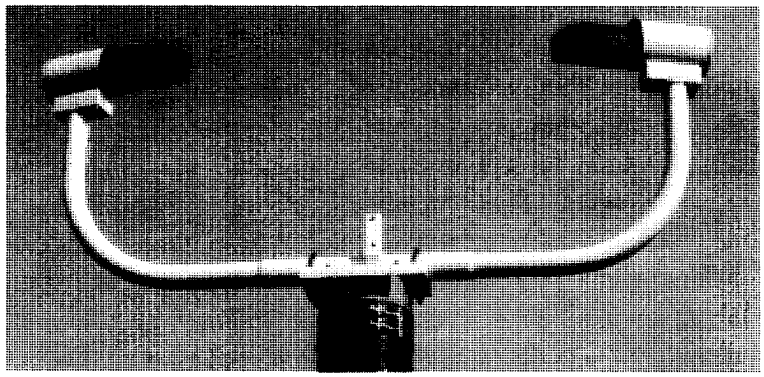

Figure 7. Handar Look-Out Scattermeter, Side View

4.2.7 Look-Down Beams

Figure 8 shows the first commercially available look-down forward scattermeter, which uses flashlamp technology. It is used in the National Weather Service's Automatic Surface Observing System (ASOS). Apart from any problems associated with looking at the ground, the look-down geometry has much to commend it:

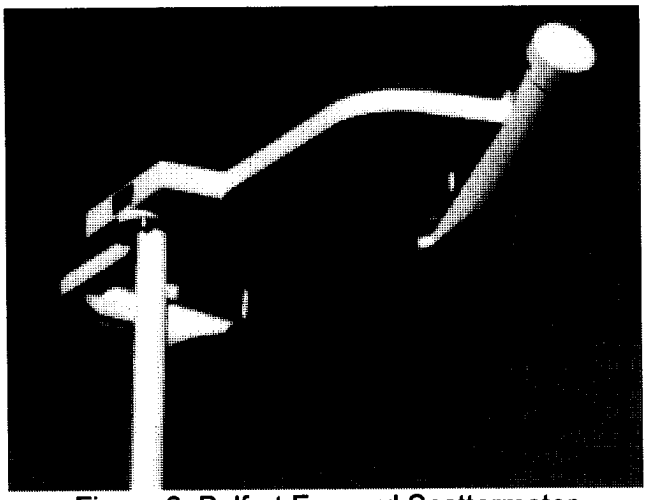

Figure 8. Belfort Forward Scattermeter

1. Blowing snow is less likely to clog the windows.

2. Dirt is less likely to contaminate the windows.

3. Any heat generated by sensor heads or hoods is above the scatter volume and will therefore not affect the fog in the scatter volume.

Note that the original EG&G forward scattermeter (Figure 3) looked partially at the ground; this orientation likely contributed to its "glint" problems. The short pulse of flashlamps and the high frequency modulation of LEDs have, however, almost totally eliminated this problem from current forward scattermeters. At present, the "glint" effect is noted for the US RVR scattermeter only under rare conditions of bright sun and heavy rain, where sunlight scattering from the raindrops may saturate the electronics.

4.2.8 Window Contamination Correction

A forward scattermeter with horizontal optics (e.g., unit shown in Figure 4) cannot meet the required FAA 90-day maintenance cycle for window cleaning (less than 10 percent window loss in 90 days); this problem was first noted in 1986 airport tests. A second related problem is how to detect when a sensor window is clogged with snow and therefore blocks the detection of scattered light; a clogged scattermeter will report good visibility when the visibility may be bad.

Two methods were devised to deal with these problems:

1. The Qualimetrics sensor (Figure 5) uses four heads, two transmitters and two receivers. Each receiver looks directly at one transmitter and sees scattered light from the other transmitter. The transmitters are operated alternately to give direct and scattered signals from each receiver. If the four signals are combined, the resulting extinction coefficient becomes independent of all sources of drift, including window contamination (as long as it is uniform on the window). The Qualimetrics sensor reliably detects snow clogging; if only one of the two transmitter or receiver heads is clogged, then it can still operate in a reduced reliability mode equivalent to a normal two-head scattermeter.

2. The Handar sensor (Figures 2, 6, and 7) uses internal scattering measurements to detect window contamination. The receiver window is illuminated at a 45° angle with an additional LED while the transmitter window is viewed at a 45° angle with an additional photodiode. This approach is less cumbersome than the Qualimetrics approach but has two limitations: (1) it cannot detect snow clogging away from the window and (2) it generates some interesting problems when water droplets are on the windows (see Section 6.1.2).

4.3 LABORATORY TESTING

The testing of extinction coefficient sensors is normally conducted in the field. However, alternative test methods have been pursued because of the many drawbacks associated with field testing, as listed below:

1. Uncertainties in the occurrence and reproducibility of the desired low visibility conditions,

2. Long turn-around times for fixing sensor problems (especially snow effects which may require delays of as much as a year before tests can be repeated),

3. Difficulties in keeping all test equipment operational for the duration of the test, and

4. Large amounts of data collected, most of which is uninteresting.

In 1982, a comprehensive test[4] involving haze, fog, snow and rain was conducted in a very large climatic chamber that could hold the standard US transmissometer (76-meter baseline). Fog with a measured extinction coefficient as large as 500 /km was generated by cooling or by injecting steam into the chamber. This fog, however, was not very uniform. Snow generated by a snow gun was also not very uniform, and may not have been a realistic representation of natural snow. Stable, uniform haze with high extinction coefficients (up to 50 /km) was generated by operating the snow gun at warm temperatures; when the fine water droplets evaporated they became haze particles because of the slight amount of salt in the water.

In 1993[8], 1995, and 1996[9] controlled chamber tests were conducted at the US Army Cold Regions Research and Engineering Laboratory to support the development of the new US RVR system. The most useful tests used a moderate sized (8 X 12 meters), temperature controlled chamber. The goals of these tests were to assess the dense fog and severe weather performance of the sensors and to devise methods for preventing snow clogging. The following conditions were generated:

Fog - was generated by steam injection and by snow gun operation under saturated conditions (maximum measured $\sigma > 600$ /km for US RVR scattermeter).

Wind, Blowing Snow - In 1995, a 6-meter long wind tunnel was built to provide uniform wind (2-15 m/s) over a square area of 0.6 X 0.6 meters. Provisions were made to inject a controlled amount of man-made snow into the wind stream.

The results of these tests are discussed in Sections 6.22 and 6.2.4.2.

4.4 US RVR SPECIFICATION

Starting in 1980, the Federal Aviation Administration, with the assistance of the Volpe Center, has worked closely with the Air Force Geophysics Laboratory (AFGL) in evaluating the performance of forward scattermeters at the AFGL Otis Weather Test Facility (WTF) on Cape Cod, MA. A report was published[10] on the 1984-1985 work. In 1983-84, an invitational test, similar to the subsequent 1988-89 WMO test[5], was conducted at the Otis WTF. The instrument models tested included: seven forward scattermeters, two back scattermeters, four transmissometers and one television system. There is no public report on this test since the results were kept proprietary to each participant.

Based on the Otis WTF test results, the FAA decided in 1985 that forward scattermeter technology was mature enough to be included in the RVR System Specification[11], which required a single point sensor. The specification defined performance requirements for the extinction coefficient sensor that were based on the test methods developed at Otis and are described in the following sections. See Section 5.2.3 for more discussion of the rationale for the test requirements.

The rationale for the accuracy requirements is to restrict systematic errors to about ± 10 percent, since systematic errors represent a bias in the resulting RVR values. Larger random errors are permitted since the other random errors in estimating RVR, such as pilot's eyesight and spatial variations in fog density, are much larger than ±10 percent.

Sections 4.4.1 and 4.4.2 are statements from the RVR specification.

4.4.1 Accuracy Requirements

The sensor shall measure the atmospheric extinction coefficient, σ, to an accuracy of ± 20 percent root-mean-square equivalent (rmse), 90 percent confidence over the range 1.5 /km to 10 /km and to an accuracy of ± 15 percent rmse, 90 percent confidence level over the remaining range of 10 /km to 300 /km. A 15 percent rmse means a normal error distribution having a standard deviation of 15 percent. The 90 percent confidence level corresponds to 1.65 times the standard deviation or 25 percent; i.e., the sensor measurement error will be less than 25 percent at least 90 percent of the time.

No more than one percent of the σ measurement errors shall be greater than a factor of two.

The sensor's mean error shall not change by more than 10 percent during any 3-month period.

4.4.2 Test Requirements

The extinction coefficient sensor must be tested and its performance must be demonstrated under the following conditions:

1. The test sensor output shall be compared to two standard FAA (reference) transmissometers. The two reference transmissometers must agree with each other within ± 10 percent of the extinction coefficient value computed from the transmittance measurements after correcting them for background error for a one-minute period for each of the tests. The "reference" is the one-minute average of the two transmissometers.

2. At least three months of data shall be accumulated. Data shall consist of a number of independent one-minute samples composed of visibilities over the dynamic range of the sensor.

3. Data shall be collected in conditions of fog, rain and snow. A minimum of five percent of the data shall be in snow, and a minimum of ten percent in rain, with the remainder in fog.

4.4.3 Calibration Requirements

Calibration requirements were added to later versions of the RVR specification. For clarity, the requirements have been simplified and restated here:

1. The fog response of a sensor when calibrated with different calibrators shall not vary by more than ± 3 percent [a specification on the consistency of the calibration process].

2. The mean fog response of calibrated sensors shall not vary by more than ± 7 percent from the value given by a visible light transmissometer [a specification on the unit-to-unit consistency of the sensors].

4.4.4 Product Validation Requirements

When the requirements of the RVR specification were implemented by the contractor for the new generation RVR system, the contractor adopted the conservative approach of validating all measurements before the RVR product was issued. If the performance of any sensor was suspect, the RVR product was declared missing. This approach was found not to match the operational requirements for RVR since missing RVR reports could force the closing of a runway. For example, since only one ambient light reading is made, a missing ambient light reading would close all runways. Thus, the system self-checks must respond to *real* sensor problems, not artifacts. For example, the estimation of window contamination loss using light scattering (Section 4.2.8, method 2) was found to give abnormally large signals from water droplets on the windows. These water droplets had relatively small effects on sensor performance, but appeared to represent unacceptable levels of window contamination. Consequently, more sophisticated processing algorithms (Section 6.1.2) had to be developed to deal with water on the windows.

4.5 DEPLOYED US NEW GENERATION RVR SYSTEM

The new generation FAA RVR system, manufactured by Teledyne Controls, was approved for deployment in August 1994. This section describes the sensors of the FAA's new generation RVR system that measure the three parameters needed to calculate RVR:

1. Extinction coefficient - *forward scattermeter*

2. Ambient light level (needed to estimate the pilot's illuminance threshold for Allard's Law) - *ambient light sensor* measures brightness of the northern sky

3. Runway light intensity (needed for Allard's Law) - *runway light intensity monitor* measures runway light current

4.5.1 Forward Scattermeter

Figure 2 shows the final design of the forward scattermeter of the US new generation RVR system. It evolved through two redesigns from the Handar scattermeter shown in Figures 6 and 7. The principle changes were:

1. Look-down scatter geometry,
2. Relocated calibrator plate to minimize sensitivity to manufacturing errors,
3. Extended, full coverage hoods with higher heater power, and
4. Precipitation mode for window loss correction.

4.5.1.1 Detachable Heads

The detachable heads of the Handar design facilitated the change in design. The heads were modified only by changing the hood design. The major change in scattering geometry was implemented by redesigning the yoke that mounts the heads. Note that all possible scattering surfaces, including the yokes and the insides of the hoods, are black to minimize multiple scattering from the sensor (Section 4.2.1).

4.5.1.2 Look-Down Design

The scattering angle was increased from 35° to 42° to provide equal snow and fog calibrations[7]. This greater scattering angle allowed the two heads to be aimed at about 19° below the horizon. At this angle, the hood can protect the windows from horizontally blowing aerosols. The heads are aimed out of the plane of the yoke by about 9° to keep the beams from hitting the yoke. The location of the calibrator plate was offset from the middle of the yoke so that the receiver beam footprint on the calibrator is larger than the transmitter beam footprint. Calibration modeling (Section 5.1.1) suggested that this design will reduce the effect of alignment and transmitter beam size errors on the sensor's fog calibration.

4.5.1.3 Removable Hoods

Figure 9 shows a closeup of the transmitter head. The hood is designed to not obstruct the transmitter and receiver beams and is open on the bottom to minimize the collection of snow. However, the hood wraps completely around the beam near the window to create a dead airspace that helps keep dirt and aerosols away from the window. The head was made removable to facilitate window cleaning.

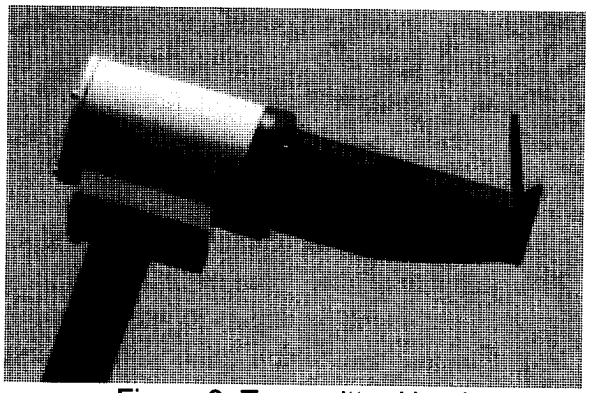

Figure 9. Transmitter Head

4.5.1.4 Calibration Plate

The large dynamic range of the scattermeter (raw

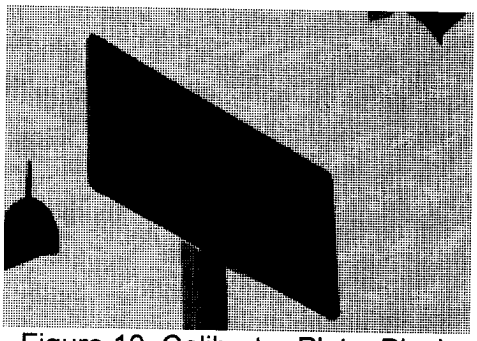

Figure 10. Calibrator Plate, Black Side

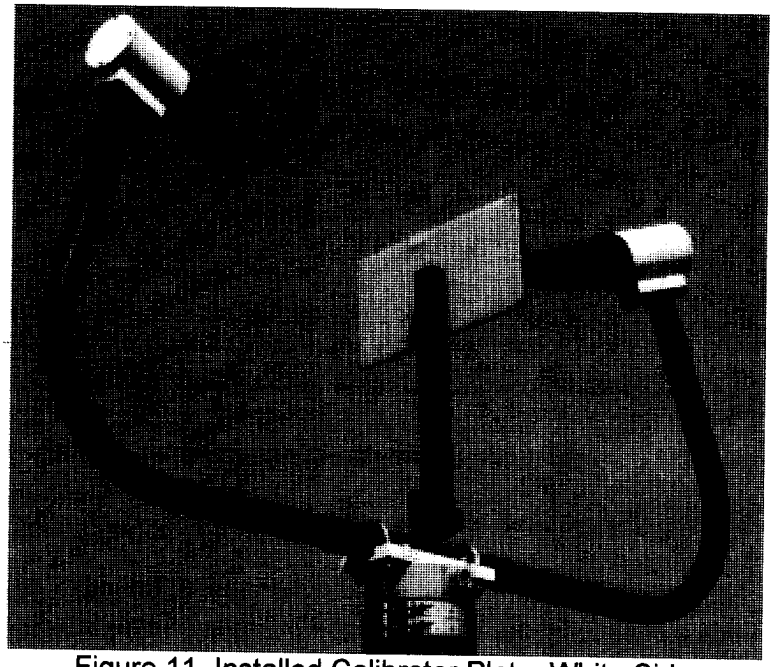

Figure 11. Installed Calibrator Plate, White Side

extinction coefficient from 0.02 to 650 /km) is achieved by using two analog ranges. The low range (0.02 to 100 /km) covers virtually all airport conditions. The high range (100 to 650 /km) serves to complete the Category IIIb and IIIc coverage of the sensor. To prevent receiver saturation, the high range is implemented by reducing the intensity of the transmitter.

Figures 10 and 11 show the scattermeter calibrator, which consists of a white plastic diffuser and a black attenuator. The attenuator contains an array of small holes that pass light. The two ends of the calibrator plate have different hole densities and hence represent different extinction coefficients; the values are set to cover the low and high analog ranges, e.g., 35 and 160 /km. The plate can be rotated to place either end in the scatter volume.

The calibration process starts with cleaning the scattermeter windows. The zero level is determined by blocking the sensor windows. Both low and high analog ranges are then calibrated using the low range of the calibration plate. The gain of the high analog range is then checked using the high range of the calibration plate.

4.5.1.5 Attenuation Correction

The original method of computing extinction coefficient from the scattermeter signal took into account the attenuation of the light beams within the sensor and hence used a more complicated calibration equation than Equation 14:

$$S = (1/K)\,\sigma \exp(-d\sigma), \qquad (14)$$

where d represents the distance between the transmitter and the receiver along the scattering path, which is approximately one meter. Note that this correction affects only the upper σ range and hence is rarely significant in airport measurements. Fog chamber tests in 1993[12] indicated that the attenuation correction was not needed and it was, therefore, removed from the national deployment sensor. This test used rapidly varying fog density and a transmissometer that was not designed for short-baseline operation.

Theoretical considerations suggest that this correction should actually use a distance d of only 0.5 meters. Half of the fog extinction coefficient represents forward scattering that does not effectively remove light from the beams. [Note that the product σd appears in Equation 14 so that reducing d by a factor of two is equivalent to reducing σ by a factor of two.] Recent field tests appear to confirm the theoretical value for the attenuation correction and its implementation is being considered for the deployed RVR systems.

4.5.1.6 Frangible Pole

The national deployment forward scattermeter is mounted on a frangible fiberglass pole that is tall enough to place the sensor at the standard United States measurement height of 4.3 meters above the runway. The base is designed so that the pole can be tilted down to service the scattermeter.

4.5.2 Ambient Light Sensor

Figure 12 shows the ambient light sensor (ALS). It is very similar in design to the scattermeter receiver. It views the sky 6° above the northern horizon and has a 6° field of view (full width). Since the look-down geometry obviously cannot be used for the ALS, it is the part of the RVR system most easily affected by blowing snow. Fortunately, the calculated RVR value is much less affected by the ambient light reading than the extinction coefficient reading. Whereas a percentage error in extinction coefficient translates approximately into the same percentage error in RVR, the RVR has a logarithmic dependence on ALS reading; that is, a factor of two (or four) reduction in ambient light gives approximately a 10 (or 20) percent increase in RVR.

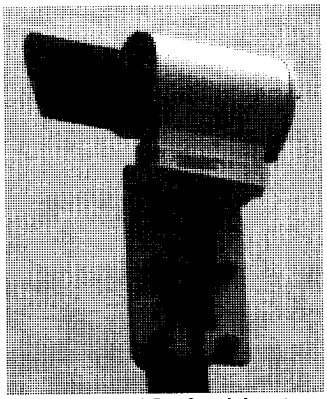

Figure 12. Ambient Light Sensor

4.5.3 Runway Light Intensity Monitor

The runway light intensity monitor (RLIM) uses a current transformer to measure the runway light current in the power vault. The measured current is interpreted as one of the six standard US runway light settings (0, 1, 2, 3, 4, and 5). The nominal runway light intensity (edge and/or centerline) for the setting is then used to calculate the RVR.

5. US RVR FORWARD SCATTERMETER CALIBRATION

The fact that the forward scattermeter is not self-calibrating like the transmissometer leads to more than half of the acceptance issues discussed in Chapter 3. This chapter addresses these issues[13] as they relate to the US RVR development. Comparisons with the measurements of transmissometers were used to determine four parameters:

1. The mean fog calibration for the scattermeter.

2. The variance in the fog calibration of the scattermeter.

3. The unit-to-unit variance in the mean fog calibration.

4. The mean snow calibration.

Before presenting these measurements it is necessary to discuss how the sensors were selected for calibration against the transmissometer. Unless the errors associated with individual sensor units are estimated, it is not possible to know how well their calibration will characterize the entire production of scattermeters. Initial deployment of the scattermeters in 1994 used the preliminary calibration presented in Section 5.3.1. Three randomly selected sensors were used for that calibration. Subsequently, the initial calibration was refined with measurements of five "golden" sensors (Section 5.3.2) having yoke parameters near nominal design and calculated calibrations near the middle of production variation.

The integrity of an RVR system requires that the calibration of each extinction coefficient sensor be known to be accurate. The following audit trail was used to assure the correct calibration for each scattermeter [the details of how calibration plates enter into this process are not included here, but were explained in Section 2.3.2.2]:

1. The yoke of each sensor was measured to verify that it meets manufacturing tolerances.

2. A calibration simulation program was used to calculate the variation in calibration from the yoke measurements for a large sample of the produced sensors.

3. A number of sensors with calculated calibrations near the median of the production variation were compared with reference transmissometers to determine the nominal fog calibration.

The details of these steps are presented in the following sections.

5.1 CALIBRATION ERROR SIMULATION

The fact that manufacturing errors lead to calibration errors was discovered in 1986 airport test comparisons with transmissometers. A calibration simulation program was written[14] to calculate the ratio of scattering (1) from the calibration plate, and (2) from fog filling the volume of overlap between transmitter and receiver beams. The only assumptions of the calculation are the angular variation of scattering from the calibration plate and fog. The calibration simulation program was used both to optimize sensor design and to evaluate manufacturing consistency.

5.1.1 Design Considerations

The first application of the calibration simulation effort was to determine how to minimize the effect of manufacturing errors on calibration variation. The errors considered included transmitter and receiver beam size and alignment, as well as calibrator location. The first design investigated utilized transmitter and receiver beams with sharp edges and identical footprints on the calibrator plate. The calibration simulation showed this design to be very sensitive to almost all manufacturing errors. Most errors changed the overlap of the beams on the calibrator plate much more than they changed the volume scattering. Two strategies were found to reduce this sensitivity:

1. Tapering the beams generally reduces the sensitivity to all errors.

2. Making the footprint of one beam larger than the other on the calibrator plate reduces the sensitivity to all but size errors of the larger beam. This strategy is therefore most effective if the beam with the most consistent size (typically the receiver) is made larger.

The national deployment sensor (Figure 2) adopted both of these design features. If beam overlap effects are minimized, the mean scattering angle becomes the most important parameter in defining the calibration because the scattering from fog decreases rapidly with scattering angle while the scattering from the calibrator decreases slowly with angle. The scattering angle must, therefore, be closely controlled to produce units with consistent calibrations.

5.1.2 Manufacturing Tolerances

The manufacturing tolerances for the national deployment yokes were defined in accordance with the calibration simulation results:

1. The scattering angle between the transmitter and receiver beam centers must be $42° \pm 0.25°$.

2. The intercepts of the transmitter and receiver beam centers on the calibrator could be displaced by no more than 7.6 mm.

These manufacturing tolerances were checked for each yoke by means of a coordinate measuring machine (CMM).

5.1.3 Calibrations Calculated from Yoke Measurements

The CMM program saves the complete yoke geometry. The calibration simulation program was rewritten to make use of actual yoke measurements rather than the hypothetical errors considered in Section 5.1.1. The calibration can then be predicted from the measurements for each yoke. Section 5.1.3.1 presents the calibration predictions for 87 yokes.

Several steps are currently underway to enhance this calibration simulation:

1. Assess the sensitivity of the results to the assumed angular dependence of the scattered intensity for fog and for the calibration plate.

2. Validate the computer code of the model.

3. Add the expected variations in head parameters (pointing angles and beam widths) to the simulation of yoke effects.

5.1.3.1 Distribution of Calculated Calibrations

Teledyne Controls analyzed the results of the CMM measurements. Figure 15 shows the distribution of calculated calibrations for 87 yokes with complete CMM geometry measurements. The nominal calibration is taken as the mean calibration for the 87 units. The distribution is well within the ± 7 percent specification. However, the effects of head variations have not been included.

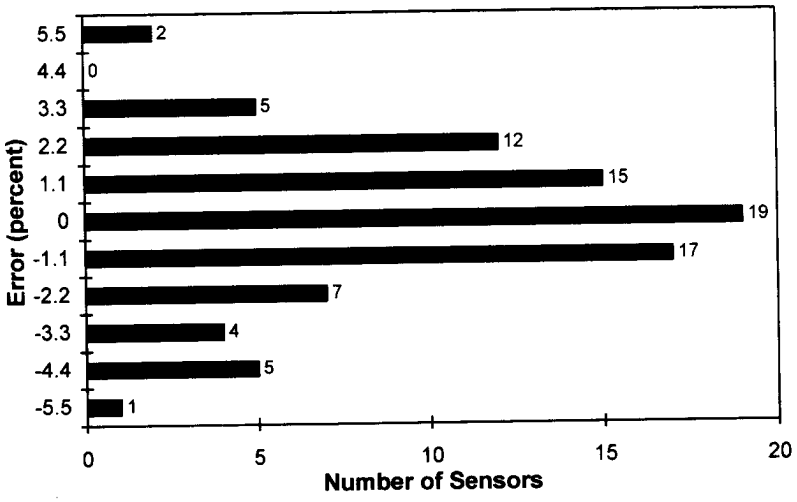

Figure 13. Distribution of Calculated Calibrations

A test of CMM measurement repeatability showed that the calculated calibration can vary by as much as ± 1 percent. Although this variation will slightly broaden the distribution, it has no significant impact on the results presented in Figure 13.

5.1.3.2 Golden Yokes

Five "golden" yokes, i.e., yokes with close to nominal geometry and calculated calibrations close to the mean, were selected for calibration testing at the Otis WTF. Table 1 lists their characteristics.

Table 1. Characteristics of "Golden" Yokes

Serial Number	Calculated Error (relative to mean)	Beam Offset at Calibrator	Scattering Angle (degrees)
107	0.04 %	5.6 mm	41.83
98	0.22 %	5.1 mm	41.89
287	1.10 %	4.1 mm	41.86
481	1.10 %	3.2 mm	41.91
201	1.10 %	4.0 mm	41.89

5.2 CALIBRATION FIELD TEST METHODOLOGY

5.2.1 Otis Weather Test Facility

Most calibration field testing has been carried out at the Otis WTF, which is located on Cape Cod Massachusetts and is operated by the Air Force Phillips Laboratory, Geophysics Directorate. The site experiences fog in every month of the year. The Otis WTF (see Figure 14) was originally instrumented with two crossed transmissometers (projector:receiver P1:R1 and P2:R2) to study fog

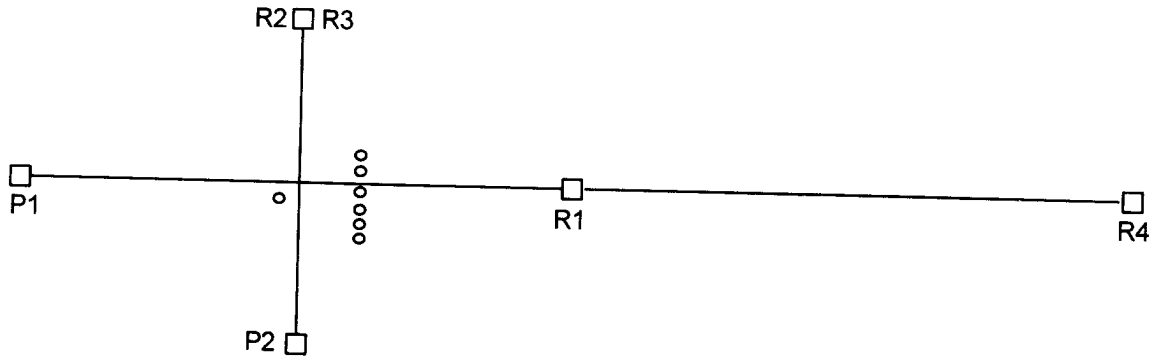

Figure 14. Layout of Otis Weather Test Facility

dispersal. Later, scattermeters were installed (small circles) near the crossing region to determine their calibration relative to the transmissometers.

5.2.2 Reference Sensors

As described in Section 2.3.2, the calibration of a forward scattermeter must be determined by comparison with reference transmissometers. The reference transmissometers at the Otis WTF are standard US transmissometers (see Section 2.2.4), but they are operated in a somewhat different manner than at airports.

5.2.2.1 Two Crossed Transmissometers

The original transmissometer installation at the Otis WTF consisted of crossed 91- and 152-meter baselines (P2:R2, P1:R1, respectively in Figure 14). Visible light filters (see next section) were installed in the receivers of both these transmissometers. The average extinction coefficient measurement from these two transmissometers is the reference standard for calibrating the US RVR forward scattermeter.

Two additional receivers (unfiltered) (R3 and R4 in Figure 14) were installed to create two additional transmissometers which use the same projectors as the original transmissometers:

1. Transmissometer P2:R3 (91-meter baseline) averages over the same volume as P2:R2 and provides a direct comparison of the fog response of filtered and unfiltered transmissometers.

2. Transmissometer P1:R4 (304-meter baseline) was originally intended as a reference for higher visibilities. It also permits the representativeness analysis described in Appendix A. The lower signal-to-noise ratio for the longer baseline precluded using a visible-light filter.

5.2.2.2 Visible-Light Filters

Since the standard US transmissometer has no optical filter in the detector, its spectral coverage is the convolution of the response of a silicon photodiode with the emission spectrum of an incandescent light. This combination gives considerable response in the near infrared. For stability and long life, the

projector lamps are operated at reduced current, which further decreases the fraction of light in the visible portion of the spectrum. The two original reference transmissometers (P1:R1, P2:R2 in Figure 14) were converted to use only visible light by installing filters blocking wavelengths longer than 0.65 microns. The loss of light intensity indicated that only 15 percent of the response of an unfiltered transmissometer comes from wavelengths shorter than 0.65 microns.

Comparisons between the filtered and unfiltered 91-meter baseline transmissometers showed the effect of including infrared light in the transmissometer measurement. In fog the extinction coefficient measured by the unfiltered transmissometer was consistently 3.5 percent greater than that measured by the filtered transmissometer. This observation is consistent with prior reports on the variation of the fog extinction coefficient with wavelength. Since visible light transmissometers are used to define the calibration of the RVR forward scattermeter, a 3.5-percent correction was used whenever comparisons were made of forward scattermeters with airport transmissometers.

5.2.2.3 Transmissometer Calibration

An automatic transmissometer calibration method is used at the Otis WTF (see Section 2.2.2 for airport calibration methods, which are different from that used at Otis). The clear days are determined by the measurements of a stable forward scattermeter with little self scatter offset (HSS VR-301B shown in Figure 4). The transmissometer calibrations are corrected whenever the scattermeter extinction coefficient is below 0.10 /km (>30 km visibility). The transmissometer offset correction is then set to give the actual extinction coefficient according to measured high-visibility slopes[7] between the transmissometer and the forward scattermeter. If the visibility is high enough, this correction is made once per hour, using a ten-minute average of extinction coefficient starting five minutes after the lamp is turned on again after being extinguished to determine the sunlight background reading. The five-minute delay eliminates turn-on transients in the lamp intensity.

5.2.3 Homogeneity Criteria

The objectives for comparing transmissometer and scattermeter measurements are to determine the mean calibration of the scattermeter and the variance between the responses of the two instruments to the obstruction to vision. Since the two instruments measure different portions of space, the variance between their readings will also depend upon the spatial homogeneity of the obstruction to vision. This variance must be minimized if the test results are to characterize the relative response of the two instruments. The issue of how well the spatial coverage of scattermeter and transmissometer measurements represent the atmosphere was discussed in Section 3.3.

All the visibility instruments at the Otis WTF are mounted at a consistent three-meter height above the ground to avoid any systematic variation in the density of the obstruction to vision as a function of height above the ground. Horizontal variations in the obstruction to vision are reduced by selecting data points when the horizontal variations are below a certain homogeneity criterion. Two homogeneity criteria have been used:

1. The two crossed transmissometers at the Otis WTF can be used to determine when the obstruction to vision is homogeneous. Their two readings must agree to within a specified percentage or the data point is rejected. Since the two transmissometers may agree randomly even under very

inhomogeneous conditions, a slightly more sophisticated algorithm is applied. The homogeneity criterion is applied to ten-minute set¬ of data. Unless more than half the points in the ten-minute interval meet the homogeneity criterion, all are rejected. If more than half meet the criterion, then those meeting the criterion are accepted. The use of transmissometer-based homogeneity criterion has a side benefit of eliminating data when one of the two transmissometers is partially clogged with snow. Note that the Otis transmissometers can be used to test homogeneity because they have different orientations. Close-spaced parallel transmissometers will sample mostly the same spatial variations and therefore will agree under very inhomogeneous conditions.

2. If only one reference transmissometer is available, its time variation can be used to assess homogeneity. A point is accepted if the transmissometer measurement of the prior point and the next point both agree to better than the specified homogeneity percentage.

5.2.4 Obstruction to Vision

At the Otis WTF the obstruction to vision is determined automatically from measurements of an optical precipitation identification sensor (HSS Model PW-401B). Fog is defined as any data point with no precipitation, i.e., precipitation rate (liquid water content) less than 0.0012 inches per hour. Rain and snow are distinguished directly by the precipitation sensor. The box plots described in the next section divide the data points into no precipitation, rain, and snow plots.

5.2.5 Data Analysis Via Box Plots

Early analyses[10] of data from the Otis WTF used scatter plots for many fog events to determine scattermeter calibration and to assess calibration consistency. A least-square straight line fit was made to the data of the scatter plot for each event to assess the best calibration and the variance of the fit.

The box plot was introduced to the evaluation of visibility sensors in the report[5] on the 1988-89 WMO tests. It provides a systematic method of combining large amounts of data from many events into a single presentation. The first presentation[15] on the performance of the new generation RVR system used both scatter plot and box plot analyses.

A systematic method was developed[16] to determine the fog, snow and rain calibration of forward scattermeters by combining appropriate MOR bins of a box plot. This method will be outlined using sample data from one golden yoke sensor (complete data will be presented in Section 5.3.2).

5.2.5.1 Fog

Figure 15 shows a sample plot for one-minute data points with no precipitation, which is the practical definition of "fog" for the analysis. The box plot is generated by defining logarithmic bins of meteorological optical range (MOR = $3/\sigma$) based on the average of the two crossed transmissometers (termed "TAVE"). Note that these bins are plotted vertically on a logarithmic axis. Within each MOR bin, the distribution of MOR ratios is calculated for the test sensor (in this case TDN1, one of the golden sensors) to the reference sensor (TAVE), which is the average of the two visible-light reference transmissometers. Several percentiles of the MOR ratio distribution are plotted. The median (50^{th} percentile) is plotted with an X. The 25^{th} and 75^{th} percentiles are plotted with a box, which gives the

name "box" to the plot. Half of the ratio distribution lies within the box. The 5th and 95th percentiles are indicated with a heavy horizontal line. The heavy lines encompass 90 percent of the data. Finally the 2.5th and 97.5th percentiles are plotted with a thin line. These thin lines were added to the original plot design to indicate the two standard deviation limits (95 percent of the data).

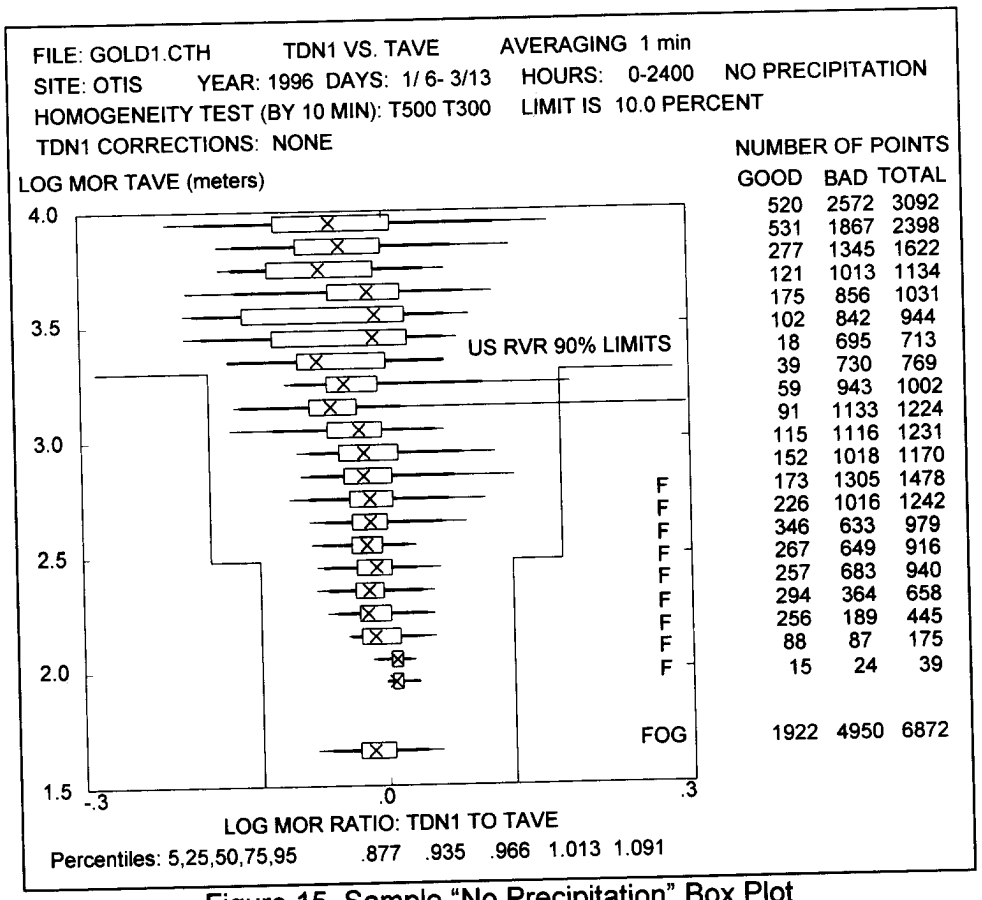

Figure 15. Sample "No Precipitation" Box Plot

The numbers at the right side of the box plot show the number of data points included in the ratio distribution (labeled "GOOD"). These are the points that passed the homogeneity test (10 percent for this sample) and had the correct obstruction to vision (no precipitation). The number of points labeled "BAD" is the number that failed the homogeneity test for the MOR bin (with no consideration of obstruction to vision). Finally, the column labeled "TOTAL" is the sum of the "GOOD" and "BAD" column. The total column is meaningful only when the selected obstruction to vision includes most of the data points, as in Figure 15. For Figures 16 and 17 that select precipitation, the fact that the "BAD" column includes all obstructions to vision makes the total column meaningless.

Up to this point, the description of the box plot in Figure 15 is essentially the same as presented[5] in the WMO test report. It is turned into a calibration method by selecting MOR bins that represent the fog calibration (marked with an "F" at the right side) and combining them into a new bin (marked with "FOG") at the bottom of the plot. The "FOG" bin includes MOR values below about 650 meters, which corresponds roughly to daytime RVR below the Category I minimum. Over the test period of three months, there were 1922 data points that met the fog calibration criteria. At the bottom of the plot the MOR ratios are listed for five percentiles. The median ratio is 0.966. The width of the box (termed Δ25-75 in later tables) is 1.013 - 0.935 = 0.078. The median ratio is taken as the best estimate of the sensor fog calibration. The width of the box is taken as an indication of the calibration variation.

The US RVR accuracy specification from Section 4.4.1 is plotted on the box plot. Ninety percent of the MOR ratios must lie within the indicated 90% limits. Since 90 percent of the ratios in each MOR bin are within the heavy horizontal lines, it is clear that, in fog, this sensor passes the US accuracy requirement by a wide margin.

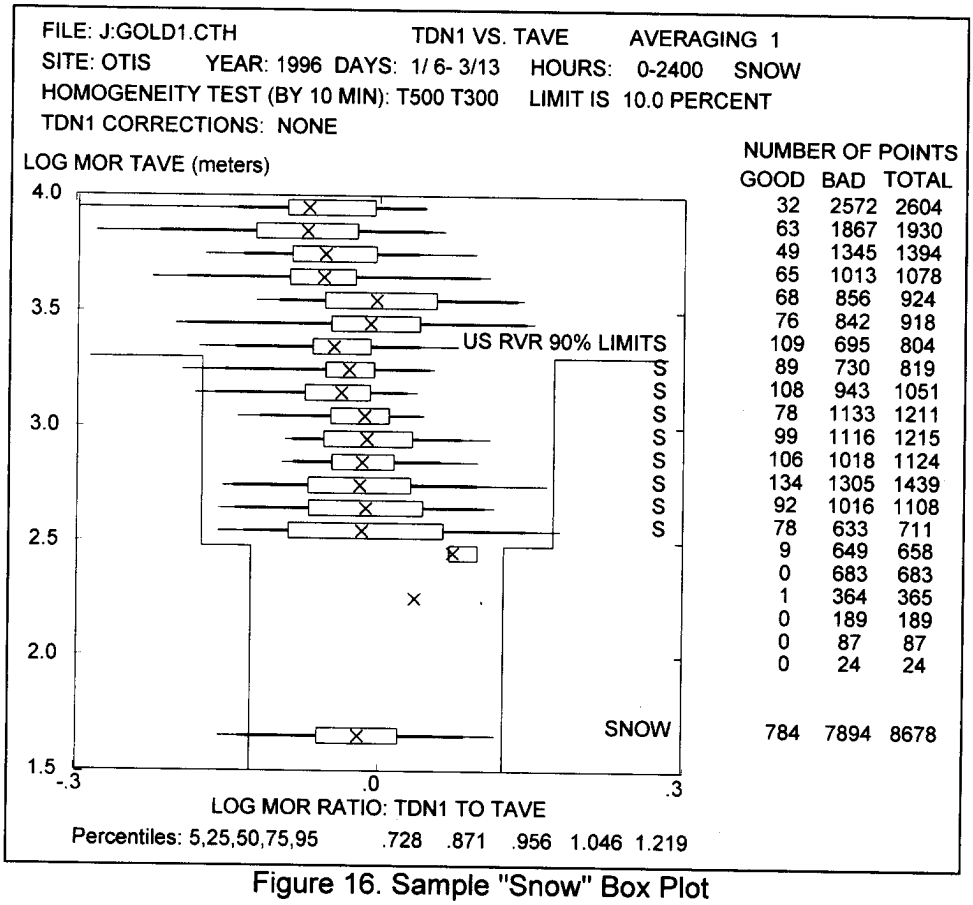

Figure 16. Sample "Snow" Box Plot

5.2.5.2 Snow

Figure 16 shows a sample snow box plot for the same test period and sensors as Figure 15. The MOR range selected for snow is 300 to 2000 meters. Snow rarely reduces the MOR below 300 meters. The median snow calibration in Figure 17 is 0.956, which is very close to the median fog calibration in Figure 15. The number of data points, however, is smaller, only 784. The box width is much larger: 1.046 - 0.871 = 0.175. This sensor meets the RVR accuracy specification in snow, but by a smaller margin than in fog.

5.2.5.3 Rain

Figure 17 shows a sample rain box plot for the same test period and sensors as Figures 15 and 16. The MOR range selected to represent rain (roughly 1500-3000 meters) requires some explanation.

First, rain without fog is rarely intense enough to reduce the visibility into the RVR region (<2000 meters). Thus, in Figure 17 most of the data points in the RVR region are for rain accompanied by fog, where the visibility is dominated by the fog component.

Second, the calibration of a forward scattermeter for pure, fogless rain is significantly different from the fog calibration[17]. The range selected in Figure 17 to represent the rain calibration was an attempt to pick out MOR values where pure rain may occur, while not straying too far from the RVR region. The scattermeter/transmissometer rain MOR calibration ratio in Figure 17 is 0.8 (0.795 rounded off), which is higher than the pure rain value of about 0.6. The difference in the pure rain and fog calibrations between the forward scattermeter and the transmissometer is actually caused by the

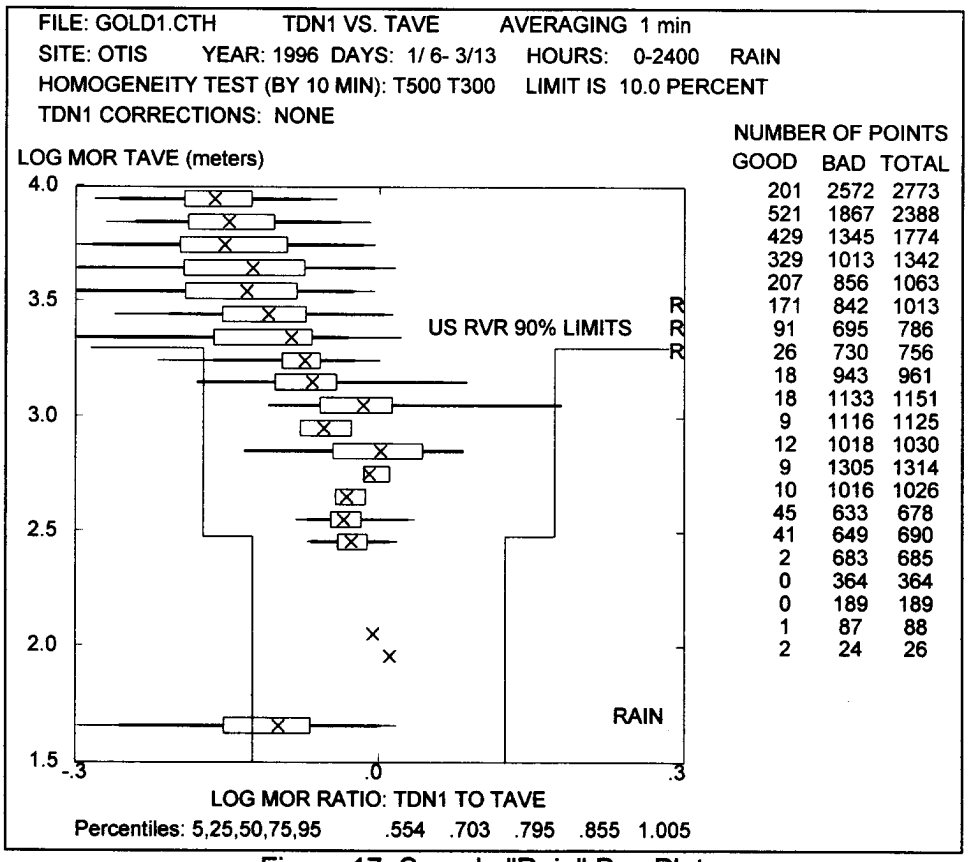

Figure 17. Sample "Rain" Box Plot

characteristics of the transmissometer, not the forward scattermeter. The reason is interesting and raises a subtle question about which instrument best represents human vision. Scattering of light from particles consists of two components, which have equal magnitudes. The first component is the light that hits the particle and is scattered into all directions. For spherical water particles, this scattering is more or less independent of particle size until the particle diameter approaches the wavelength of light. The second component is the hole left in the incident light field because of the light removed by the particle. This hole causes diffraction scattering in the forward direction; the typical scattering angle is proportional to the ratio of the wavelength of light to the particle size. This scattering angle is less than the scattering angle of a forward scattermeter for both fog and rain; thus, the scattermeter responds primarily to the direct scattering. The diffraction scattering angle in fog is much greater than the angular spread of the transmissometer beam; therefore, the transmissometer measures all the scattering from fog. However, the diffraction scattering angle for rain is typically smaller than the angular spread of the transmissometer beam; diffraction scattering from rain is therefore only partially detected by a transmissometer. Thus, the transmissometer does not measure the total extinction coefficient in rain. This difference between the transmissometer and the forward scattermeter results in a higher rain extinction coefficient from the scattermeter than from the transmissometer when the scattermeter has been calibrated to agree with the transmissometer in fog.

How significant is the difference in rain response between the transmissometer and the forward scattermeter?

1. The 0.6 MOR ratio in pure rain is outside the US RVR accuracy specification. If the test period includes a significant amount of pure rain, the forward scattermeter could fail to meet the accuracy criteria. The test period shown in Figure 17 would not have this problem, however.

2. Since the transmissometer is not correctly measuring the total extinction coefficient, one could argue that the forward scattermeter value is a more accurate measurement. However, one can also make the case[17] that the transmissometer is ignoring a component of the scattering that does not degrade human vision. In this case, the transmissometer is making a "correct" error.

3. If the transmissometer reading is correct, then the forward scattermeter is making a conservative error; the reported RVR in rain would be lower than given by a transmissometer. One could argue that such a conservative value is appropriate since the normal RVR equations do not take into account, for example, the effect of rain on the windscreen in degrading a pilot's vision.

4. In any case, pure rain typically does not reduce the RVR below the Category I minimum.

5.3 CALIBRATON RESULTS

A preliminary calibration was determined before the national deployment sensors were commissioned for airport use. Subsequently, the measurements on "golden" sensors (Section 5.1.3.2) were used to refine the preliminary calibration.

5.3.1 Preliminary Fog Calibration

Table 2. Preliminary Calibration Sensors

	Serial Numbers			
Name	Yoke	Rx Head	Tx Head	Minutes
TDN1	407	714	734	455
TDN2	360	636	622	107
TDN5	389	694	715	84

In June 1994, the three national deployment forward scattermeters listed in Table 2 were installed at the Otis WTF. Data from the fog events in June were used to derive a preliminary calibration for the sensors. The minutes of data listed in the table are for a 10-percent homogeneity criterion and are different for the three sensors because they were installed at different times.

The master calibrator (S/N 22) was measured in the three sensors listed in Table 2. Its nominal calibration value was adjusted (final value = 33.5 /km) to give the best fit to the fog calibrations of the three sensors with respect to the average of the crossed visible light reference transmissometers (Section 5.2.2.1). The first calibrators used at airports were then measured in the same three sensors after they had been calibrated by the master calibrator.

Table 3. Preliminary Calibration Check

Sensor	Minutes	Median MOR Ratio
TDN1	1244	1.050
TDN2	1315	1.009
TDN5	938	1.038

The preliminary calibration was checked in January 1995 by analyzing additional data (period 7/16/94-12/21/94) from the same three sensors listed in Table 2. The results are presented in Table 3. Although the longer test period suggested a possible change in calibration of about three percent, no changes were made until the golden yoke sensors could be tested. The sensors used for the preliminary calibration did not have complete CMM measurements and therefore their positions within the calibration distribution (Figure 13) were not known.

5.3.2 *"Golden" Sensor Fog Calibration*

Data will be presented from two test periods: 1/6/96 - 4/28/96 and 4/29/96 - 8/14/96. Two Teledyne RVR systems were installed at the Otis WTF during these test periods:

1. A standard national deployment baseline (NDB) system with a single data processing unit (DPU) connected to six sensor interface electronics (SIE) boxes in the field. One SIE controlled an ambient light sensor while the other five SIEs controlled forward scattermeters. The five golden sensors were initially interfaced to the five NDB SIEs.

2. A prototype system designed to evaluate preplanned product improvements (P^3I) to the deployed RVR system. In order to facilitate rapid software development, the prototype system uses IBM PC compatible hardware and software. The prototype SIEs are capable of operating one ambient light sensor (ALS) and one forward scattermeter. Eventually three prototype SIEs were installed, each with one scattermeter and one ALS.

Both systems use the same sensor heads. Since the most important characteristics of the forward scattermeter are defined by the sensor heads, not the controlling electronics (i.e., the SIE), the calibration data from both systems will be presented.

The selection of the five "golden" sensors was described in Section 5.1.3.2. Table 4 lists the seven Teledyne visibility sensors that were installed at Otis during the test periods. The five national deployment (NDB) units are termed TDN1 through TDN5. The three P^3I units are termed TVS1 through TVS3. One sensor (yoke S/N 107) was switched from NDB to P^3I during the first test period. The calibrations calculated from CMM data are listed in the last column. Two measurements were made for some yokes. The calculated calibrations are equal to 1.00 ±0.02. All the Teledyne scattermeters at Otis were calibrated with calibration plate S/N 22.

Table 4. Teledyne Visibility Sensors

Sensor Name		Serial Numbers			
NDB	P^3I	Yoke	Rx Head	Tx Head	CMM Cal.
TDN1		287	455	295	1.010
TDN2	TVS3	107	262	202	1.000
TDN3		98	122	158	1.017/1.002
TDN4		201	297	257	1.018/1.011
TDN5		481	865	906	1.011/0.978
	TVS1	365	486	548	N/A
	TVS2	224	333	275	0.997

Figure 18 shows six of the seven forward scattermeters after a major northeaster snow storm on 1/8/96. The two sensors on the left (TDN4, TDN3) have been rotated by 45° to the west and east, respectively, after the storm to assess the effect of wind direction on fog and snow performance.

Table 5 shows the results of the analysis where data points with no precipitation and meteorological optical range (MOR) below 650 meters were selected to represent "fog" conditions (see fog MOR range shown in Figure 15). The two test periods are included and two homogeneity criteria are shown, 10 and 20 percent. About one fourth and one sixth of the data points are lost for the first and second periods, respectively, when the homogeneity criterion is reduced from 20 to 10 percent. Note that the minutes of data vary for different sensors because of sensor malfunctions or relocations. Details of the analysis method are presented in Appendix B.

Figure 18. Row of Teledyne Visibility Sensors at Otis WTF (right to left, TDN2, TVS2, TVS1, TDN5, TDN3, and TDN4)

Table 5. Fog Calibrations of Golden Teledyne Sensors Using TAVE as Reference

		10-Percent Homogeneity			20-Percent Homogeneity		
Sensor	Period	Minutes	Median	Δ 25-75	Minutes	Median	Δ 25-75
TDN1	1	2056	0.960	0.080	2608	0.967	0.083
TDN2	1	694	0.985	0.075	1083	0.977	0.064
TDN3	1	2054	0.956	0.096	2606	0.969	0.119
TDN4	1	1483	0.997	0.117	1988	1.015	0.119
TDN5	1	2064	1.004	0.080	2598	1.011	0.089
TVS1	1	2218	1.018	0.065	2766	1.012	0.066
TVS2	1	2222	0.996	0.063	2772	0.994	0.061
TVS3	1	228	0.921	0.141	306	0.923	0.139
TDN1	2	5816	0.946	0.084	6767	0.946	0.087
TDN3	2	4727	0.935	0.075	5567	0.935	0.079
TDN4	2	5816	0.936	0.089	6767	0.936	0.093
TDN5	2	4015	0.954	0.085	4698	0.954	0.088
TVS1	2	5814	0.956	0.091	6765	0.956	0.097
TVS2	2	5811	0.959	0.102	6739	0.959	0.106
TVS3	2	2672	0.954	0.088	3004	0.956	0.093

5.3.2.1 Median Calibration

The different homogeneity criteria have only a small effect (0.018 maximum change) on the median calibrations for the first test period and virtually no effect for the second period. The different sensors have only a 2.5 % total calibration variation (0.935 - 0.959; 0.954 median value) for the second test period. The first test period (excluding TVS3 from the analysis because of the small amount of data) shows more variation, 6.4 %, from sensor to sensor (0.956 - 1.018 for 10-percent homogeneity) and a 4.2 % higher median value for the different sensors (0.996 for 10-percent homogeneity). The somewhat different calibration results for the two test periods likely reflect a different distribution of fog characteristics for the two periods (see Section 5.3.2.3 for more discussion). The smaller sensor-to-sensor variation in median calibration for the second period (2.5 % versus 4.2 %) has two possible explanations: (1) more consistent fog characteristics, and/or (2) the much larger number of data points.

5.3.2.2 Calibration Spread

The column labeled "Δ 25-75" in Table 5 is the difference between the 25th and 75th percentiles of the calibration ratio distribution; in other words, it is the width of the box in the box plot. In almost all cases spread is less than ±5 percent. In most cases, the calibration spread is slightly larger for the 20-percent homogeneity criteria than for the 10-percent homogeneity criterion, as would be expected. The spreads show more variability from sensor-to-sensor during the first test period than during the second. This observation is again consistent with more consistent fog and more data points for the second test period. Moreover, the variation appears not to be related to particular sensors; for example, TVS2 has the lowest variability in the first period and the highest in the second.

5.3.2.3 Wind Direction Dependence

In order to study the wind direction dependence of scattermeter response, a box plot was designed that plots boxes for 10-degree wind direction increments. Points are selected for MOR below a certain value (e.g., 300 meters) and wind speed above a certain value (e.g., 3.5 knots). The wind-direction box plot could be expected to detect the wind shadowing effects discussed in Section 4.2.3.

Wind shadowing effects may occur if a head support is located upwind of the scatter volume. Table 6 indicates the wind directions and the sensors with possible shadowing effects for the two test periods. The wind directions with fog were significantly different for the two test periods and may account for the differences in scattermeter performance noted in the previous two sections. The wind directions for fog did not lead to shadowing of the scattering region for the north-oriented yokes. Shadowing effects for the rotated sensors (Table 6) were at most two to three percent.

Table 6. Wind Directions for Fog

Period	Directions	Possible Shadowing
1	NE, SE-NW	TDN3, TDN4
2	SE, S-W	TDN3

The angular variations in calibration were difficult to analyze for the first test period, which included wind directions from the northeast and southeast through northwest. The detailed results depended upon the selected homogeneity criterion:

1. For 20-percent homogeneity, angular variations in median calibration of perhaps ± 7 percent were noted. The angular pattern for different sensors was generally similar, but some wind directions showed shifts in the pattern as large as four percent.

2. The calibration variance was less for 10-percent homogeneity, perhaps ± 5 percent. At some angles, the tighter homogeneity criterion eliminated 90 percent of the data points and resulted in a calibration shift as large as 10 percent.

These results can be understood as the effects of different fog types with different scattermeter calibrations. The different fog types appear to be separated by selecting wind direction and homogeneity criterion. This result is not surprising since the distance to the ocean (typically the source of advection fog) from the Otis WTF varies widely with direction.

The results for the second test period were much more consistent, both from sensor to sensor and for different wind directions.

The median sensor calibrations of Section 5.3.2.1 represent an average over the different types of fog occurring during the test period. The angular results suggest that the two test periods experienced significantly different fogs. This difference may account for the observed difference in median fog calibration for the two periods.

5.3.3 "Golden" Sensor Snow Calibration

5.3.3.1 Median Calibration

The snow calibration includes data points with MOR between 300 and 2000 meters (see snow MOR range shown in Figure 16). Table 7 shows the snow calibration results for the first test period; the second test period, of course, had no snow. Table 8 shows the ratio of the snow calibration (Table 7) to the fog calibration (Table 5). This ratio reflects the difference in the inherent scattermeter response to snow and fog with the unit-to-unit calibration variation removed.

Before discussing the ratios in Table 8, it should be noted that the snow calibration for TDN2, the sensor showing one of the lowest snow calibrations, is affected by the significant offset (0.2 /km) noted for this sensor. This offset reduces the MOR for this sensor. None of the other sensors had significant offsets during this test period.

The ratios in Table 8 range from 0.938 (TVS1) to 1.006 (TDN5). The data, therefore, suggest that the MOR calibration in snow is about three percent lower than the MOR calibration in fog. If the fog calibrations in test period two were used to calculate the ratios, the snow and fog calibrations would be equal. Considering the snow calibration spread (±9 percent) and the fog differences between the two test periods, one must conclude that the snow and fog calibrations are effectively the same. Before the increase in scattering angle from 35° to 42°, the snow MOR calibration was about 30 percent higher than the fog MOR calibration[8].

5.3.3.2 Calibration Spread

The calibration variation is much greater in snow (±9 percent) than in fog (±4 percent). The greater

Table 7. Snow Calibrations of Teledyne Sensors Using TAVE as Reference

	10-Percent Homogeneity			20-Percent Homogeneity		
Sensor	Minutes	Median	Δ 25-75	Minutes	Median	Δ 25-75
TDN1	870	0.948	0.178	1098	0.950	0.188
TDN2	420	0.927	0.134	502	0.934	0.149
TDN3	869	0.936	0.183	1097	0.944	0.196
TDN4	873	0.962	0.137	1134	0.970	0.153
TDN5	877	1.009	0.182	1127	1.017	0.195
TVS1	880	0.955	0.180	1124	0.958	0.196
TVS2	881	0.982	0.185	1124	0.993	0.201
TVS3	450	0.947	0.185	596	0.958	0.194

Table 8. Snow-Fog Ratio of Median Calibration

	Homogeneity	
Sensor	10 %	20 %
TDN1	0.988	0.982
TDN2	0.941	0.956
TDN3	0.979	0.974
TDN4	0.965	0.956
TDN5	1.005	1.006
TVS1	0.938	0.947
TVS2	0.986	0.999

snow variation can have three possible explanations:

1. The range of scattering characteristics could be larger for snow than for fog, or

2. The size of the projected area of the scatter volume is too small to properly average the snow measurement, or

3. The inherent sensor noise is more important for snow than fog since the typical extinction coefficient is smaller for snow than for fog (compare Figures 16 and 15).

If the first explanation is true, then intercomparisons between two scattermeters should give significantly less spread than the comparison between the scattermeter and the transmissometer. Table 9 compares the spreads observed using TAVE and TVS2 as references. At best a small reduction in spread is noted. Moreover, the higher signal-to-noise ratio expected for the TVS sensors appears to make no significant difference in the snow spread.

Table 9. Comparisons of Snow Spread

Sensor	vs. TAVE	vs. TVS2
TDN1	0.178	0.138
TDN2	0.134	0.105
TDN3	0.183	0.174
TDN4	0.137	0.158
TDN5	0.182	0.164
TVS1	0.180	0.180
TVS3	0.185	0.145

Another scattermeter with a larger scatter volume and a higher signal-to-noise ratio showed much smaller spreads against TAVE (less than ±5 percent). A slight reduction for scattermeter intercomparisons was also noted.

One can conclude that the large snow spread observed for the US RVR scattermeter is likely due to its small scatter volume.

5.4 CALIBRATION SUMMARY

The calibration test results show acceptable forward scattermeter performance with respect to the calibration issues listed in Section 3.1:

1. Under the ideal test conditions of the second test period, the calibration consistency of the golden sensors is good to better than ± 1.5 percent.

2. The calculated calibration variation for 87 forward scattermeter yokes is less than ±6 percent.

3. In a typical comparison between a forward scattermeter and the reference transmissometers, the spread in calibration (half the data points) is less than ±5 percent.

4. Shadowing effects of the yoke arms on the fog calibration appear to be at most a few percent.

5. The snow and fog calibrations are effectively equal for the current scattering geometry of the Teledyne visibility sensor. The typical calibration spread in snow is less than ±10 percent.

The calibration testing showed the following calibration variations:

1. Studying the fog calibration as a function of wind direction and homogeneity appears to isolate fogs with different scattering properties. The maximum observed variation in median fog calibration was ± 7 percent (first golden test period).

2. The fog calibration varied by four percent between the two golden test periods. The fog characteristics appeared to be somewhat different during the two test periods.

3. No change in the preliminary Teledyne visibility sensor calibration can be justified at this time. The preliminary calibration is accurate according to the first golden test period but four percent low in MOR for the second golden test period. Note that the preliminary calibration check in Table 3 for unmeasured sensors suggested that the preliminary calibration is about three percent high in MOR. The yokes (Table 2) used for that calibration need to be measured with the coordinate measuring machine before the relative importance of the three different calibrations can be determined.

6. EFFECTS OF PRECIPITATION ON US RVR SYSTEM

6.1 WINDOW SIGNALS

Correction for window losses are needed to meet the FAA 90-day maintenance requirement. The national deployment forward scattermeter adopted the second window loss strategy discussed in Section 4.2.8, namely scattering light from the contamination on the sensor window and estimating the corresponding window loss. This correction is applied to both scattermeter windows and the ALS window. If the window loss is L, the relationship between the raw and corrected measurement is:

$$M_{CORRECTED} = M_{RAW}/(1\text{-}L). \qquad (12)$$

Two correction factors are required, of course, for the scattermeter: one for each window. The correction in Equation 12 is reasonable when the loss L is much less than one, but becomes very sensitive to errors in L as L becomes greater than 0.5.

6.1.1 Dirt

For window contamination with dirt, the window loss L is assumed to be proportional to the window scattering signal W,

$$L = K\,W, \qquad (13)$$

and was found to be quite consistent for different kinds of dirt as long as L is less than 0.2. The US RVR system informs maintenance personnel that cleaning is needed when L exceeds 0.2 and shuts down the sensor when the value of L is above a maximum allowed value.

The window signals were recorded at four airports for one to two years where the windows were cleaned quarterly. For the forward scattermeter, the typical maximum observed value of L from dirt was less than 0.10, with an absolute maximum of 0.16. Larger values were seen for the ALS, which has a more exposed window.

6.1.2 Water Droplets

Water droplets from blowing rain or snow can produce window signals much larger than those observed from dirt. In this case, however, the relationship between window loss and window signal is much different from that given by Equation 13. For example, window droplet signals can be observed for which Equation 13 predicts losses much greater than one, which is impossible. Such signals automatically shut down the sensor since they will be above the maximum allowed value.

The water droplet problem had to be solved in order to keep the sensors on line during blowing rain or snow. The look-down geometry dramatically reduced the water droplet problem for the scattermeter, but the ALS is readily affected by snow or rain. Moreover, since there is only one ALS for all runways, a failing ALS shuts down the entire RVR system.

The resolution of the droplet problem involved two changes:

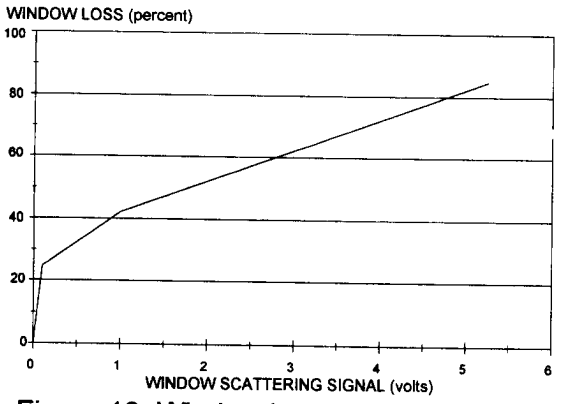

Figure 19. Window Loss versus Window Signal for ALS

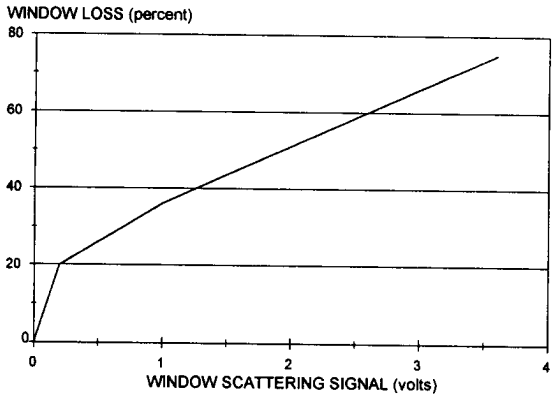

Figure 20. Window Loss versus Window Signal for Scattermeter Transmitter

1. A nonlinear equation consisting of three line segments was used to replace Equation 13. Figures 19-21 show the nonlinear relationships selected for the ALS, scattermeter transmitter and scattermeter receiver, respectively. The effect of large window signals on window loss is less than that of small window signals. The first segment of the curves is just the linear relationship of Equation 13. These curves were developed by spraying water on the windows and selecting a relationship that gives a conservative measurement; i.e., errors are biased toward higher measured values and hence lower RVR value.

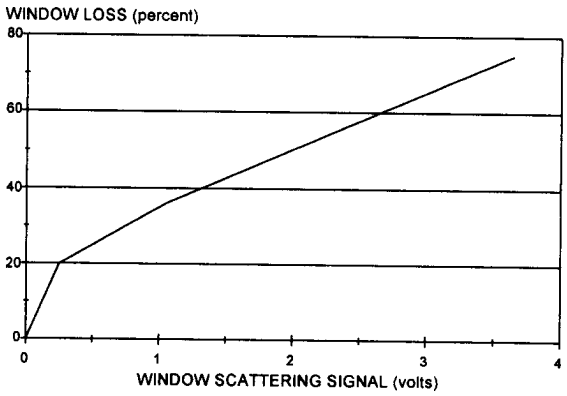

Figure 21. Window Loss versus Window Signal for Scattermeter Receiver

2. High window loss alarms are disabled when the window signals are caused by water droplets from precipitation. Water droplet signals can be distinguished from dirt signals because they vary rapidly in time.

6.2 SNOW CLOGGING

Snow accumulating on a forward scattermeter can affect its performance in two ways:

1. If the beams are blocked, the measured extinction coefficient will be too small and the reported RVR value will be too high (a non conservative error).

2. If the snow produces a multiple scattering path between the transmitter and receiver (termed "bridging"), then the measured extinction coefficient will be too large and the reported RVR will be too small. This conservative error is the same produced by a clogged transmissometer.

Although both error types are undesirable, the beam blockage has a more severe operational impact.

6.2.1 Field Test Results

Snow clogging of forward scattermeters with horizontal beams is regularly observed in severe snow storms. For example, all such scattermeters, as well as all the transmissometers, were affected by the northeaster at Otis on 1/8/96 (see Figure 18). In stark contrast, none of the look-down forward scattermeters (seven national deployment units - Figure 2 and four Belfort units - Figure 10) were affected at all. In fact, no significant window signals were observed on the national deployment scattermeters during the many snow storms of the 1995-96 winter, even after one sensor was turned to face the prevailing northeast winds. Otis experienced 30 snow days after the sensors were reoriented.

Scattermeter window signals during snow storms were studied also at four other test sites for the winter of 1995-96; Table 10 summarizes the snow data evaluated. One snow event with significant window signals was noted at each site; a significant window signal event was defined as a window loss greater than 10 percent lasting for more than a few minutes. The rarity of significant window signals is due to the look-down geometry. Many more significant window signal events were observed with the earlier look-out geometry of Figures 6 and 7. Similarly, significant ALS window signals from blowing snow are common.

Table 10. Snow Test Sites

Site	Code	Period	Snow Days
Buffalo, NY	BUF	3/15/96 - 4/18/96	17
St, Johns, NF	YYT	1/28/96 - 4/30/96	46
Kansas City, MO	MCI	10/1/95 - 4/30/96	29
Denver, CO	DIA	9/1/95 - 4/30/96	45

Table 11. Details of Snow Events with Significant Window Signals

Code	Date	Head Angle	σ /km	SAO Time	SAO Visib. (miles)	SAO Obstruction	SAO Temp (deg F)	Wind Angle (deg)	Wind Speed (knots)	Wind Gust (knots)	Max Loss (%)
BUF	3/20/96	80°	0.8	0406	2.5	S-	36	40	22	30	22
YYT	2/7/96	350°	12	1200	.13V	S-BS	19	10	20	33	27
MCI	1/18/96	350°	2-6	1238	2	S-	6	320	22		13-28
				1355	0.5	S-F	5	330	20		
DIA	10/23/95	350°	7-9	0022	0.5	SF	31	330	27	41	26-32
				0153	0.25	S+F	30	340	22	39	

The details of the significant window signal events are listed in Table 11. The weather conditions were obtained from the Surface Aviation Observation (SAO) reports. All the events in Table 11 were for the receiver. All had maximum window losses reaching into the nonlinear response region of Figure 21, but showed no indication of snow clogging. It should be noted that, during these events, at any given time some scattermeters showed window signals while others did not. The wind speed for all events was 20 knots or greater. The wind direction was within 40° of the head angle for each event. The temperature range of the events (5 to 36° F) varied from well below freezing (32° F) to just above freezing.

6.2.2 Laboratory Testing

Laboratory tests were conducted using the wind tunnel described in Section 4.3. The goals of these tests were to:

1. Determine the thermal characteristics (heater-induced temperature rise versus wind speed and direction) of the two optical sensors (scattermeter and ambient light sensor) of the US RVR system.

2. Determine how the two sensors clog in blowing snow.

3. Determine conditions of wind speed/direction and snow density leading to snow clogging of the two sensors.

4. Develop methods for reducing the susceptibility of the two sensors to snow clogging.

The test results for the forward scattermeter are presented in the following sections. The results for the ambient light sensor are presented in Section 6.2.4.

6.2.2.1 Temperatures

The critical component of the scattermeter for snow clogging is the window. Since the window heat is applied from the edges, the coldest point of the window is its center. The temperature rise above ambient of the window center depended on both wind speed and wind direction. In a 20-knot wind, the lowest temperature rise observed (i.e., worst case) for different wind directions was 20° C. Thus, natural conditions will occur when the window center will be below 0° C and window icing may occur. The coldest part of the sensor near the window is the edge of the flange around the window; the worst-case temperature rise was only 12° C in a 20-knot wind.

6.2.2.2 Blowing Snow

When snow was introduced into the wind tunnel air stream, water droplets were formed on the window for wind angles of less than about 50 degrees from the hood direction. If the temperature of the window center was below freezing, ice would form there to such an extent that significant sensor errors were probably induced; the actual window loss errors could not be measured.

Turning off the de-ice heaters on the hood and window prevented all ice formation and could be an attractive strategy for preventing heater-induced icing under dry snow conditions. However, when the heat was turned off while snow particles were being successfully melted into droplets on the windows, the resulting frozen droplets gave an unacceptable reduction in the measured extinction coefficient of the calibrator.

6.2.3 Forward Scattermeter Snow Clogging Conclusions

The laboratory tests indicated that:

1. The forward scattermeter will *always* experience window signals in blowing snow when wind of sufficient speed is within 45° of the head pointing angle. The field tests confirmed this angle response, but showed a low probability for the occurrence of window signals. The wind tunnel observations may be influenced by turbulence and by the icy nature of the man-made snow, which was prone to bounce off the sensor hood (or even the bottom of the tunnel) onto the window surface.

2. Window clogging by snow will occur only for a narrow band of temperatures, where part of the sensor or window is above freezing and another adjacent part is below freezing.

Since no signs of window clogging have ever been seen in the field for the national deployment forward scattermeter, window clogging appears to be rare or nonexistent. The scattermeters will be monitored in the future at sites where snow clogging could occur, based on the climatology of wind and snow[18].

6.2.4 ALS Performance

The ambient light sensor (described in Section 4.5.2) has much more difficulty with snow clogging than the forward scattermeter, in spite of its less stringent accuracy requirements. An error of a factor of two starts to be a problem and more than a factor of four is a serious problem (except at night where no light is measured).

6.2.4.1 Field Tests

Although field tests commonly show large ALS window signals, serious clogging has been rare. When the window is successfully melting all impinging snow, the window signals fluctuate rapidly as the number and size of droplets is continually changing. The signature of a clogged window is an increase to a steady window signal that slowly decays. Two natural window clogging events have been observed:

1. The first[8] occurred at St. Johns in 1994 with a windspeed of 30 knots and a temperature of -7° C. The clog occurred after fifteen hours of snow blowing onto the sensor window.

2. The second occurred in the 1/8/96 snowstorm at Otis where one of the ALSs was pointed into the northeast wind. Although this clog occurred before dawn, it lasted long enough that an ambient light reduction by a factor of six could be determined by comparisons with unclogged sensors (pointing north). It should be noted that the clogged sensor was controlled by a P^3I SIE (see Section 5.3.2) which provided somewhat less heater power than the national deployment NDB SIEs. The P^3I SIE heater power cycled during the storm while the NDB SIE did not.

6.2.4.2 Laboratory Tests

The CRREL laboratory tests (Section 4.3) explained the snow clogging mechanism for the ALS. When the window can no longer melt all impinging snow, slush builds up at the bottom of the window. Simultaneously, melted snow begins to refreeze on the unheated, cold face below the window. Eventually these two ice regions merge and the opening in front of the window fills with snow and ice. If this process continues to completion, the ambient light reading is readily reduced by more than a factor of ten. Moreover, because the ice clog is supported by an unheated surface, recovery from the clog can take a very long time in spite of the large amount of heat on the hood and the window. Once the ice melts away from the window, the window heat has little effect on melting the clog.

Temperature profiles were measured for the ALS. However, the dry window center temperature appears to have less impact on the clogging problem than the amount of heat available to melt

impinging snow. Clogging was observed whenever the internal window flange temperature dropped much below 10° C, whether caused by wind cooling or snow melting.

Two methods were investigated for reducing the susceptibility of the ALS to snow clogging:

1. An additional heater was applied to the sensor face around the window. This modification gave some improvement in resistance to clogging, and dramatically improved the speed of recovery from a clog.

2. An unheated aluminum box, with an opening for the ALS field of view, was placed around the ALS to reduce the wind cooling and amount of snow hitting the sensor. The box was very effective in preventing snow clogging except when the wind angle was less than 15° from the sensor axis; in this case the opening permitted the wind and snow to impinge directly on the window.

6.2.4.3 ALS Conclusions

Although ALS clogs are a demonstrated problem, the frequency of occurrence has been low. The occurrence rate will be monitored and the two mitigating methods tested at CRREL will be implemented:

1. The face heater will be added to the fielded ALS units in the future to speed recovery from a clog.

2. If necessary, airports experiencing clogging problems will be provided with instructions for constructing protective boxes.

7. CONTINUING WORK

Although the testing to date has validated the new generation RVR system, some activities are continuing to further improve and better document system performance.

7.1 CALIBRATION REFINEMENT

The existing forward scattermeter calibration will be refined by:

1. Collecting more calibration data on the "golden" sensors.

2. Validating and improving the calibration simulation program by (1) comparing calculated and measured calibrations for scattermeters with large calibration errors, (2) validating the calibration simulation computer code, (3) studying the sensitivity of the results to the assumed scattering properties of the calibration plates and fog, and (4) including head errors in the simulation.

3. Evaluating any long-term drift in sensors or calibration plates by periodically comparing the forward scattermeter calibration against reference transmissometers over the 20-year lifetime of the system. This long-term commitment is the price of using an extinction coefficient sensor that is not self-calibrating.

7.2 RARE METEOROLOGICAL CONDITIONS

Additional sensor performance data will be collected under rare meteorological conditions. In the case of snow, data will be collected to assess what "worst case" conditions can lead to sensor performance problems. If funding is available, special tests will be conducted to assess forward scattermeter performance and calibration in dust and smoke, where absorption can be important. A dust test would likely be conducted at an airport in the southwest United States. Since natural smoke is unpredictable, and generating smoke is environmentally unacceptable, smoke tests may require the use of a chamber or calculations based on prior data.

7.3 MONITORING OPERATIONAL PERFORMANCE

Data recording will continue at selected operational locations to assess sensor problems and identify other system anomalies that may not be detected by the system self-checks. Of particular concern are forward scattermeter and ALS problems in severe snowstorms, as discussed in Chapter 6.

8. CONCLUSIONS

1. Chapter 3 listed five issues that needed resolution before a forward scattermeter can be considered validated for use as the extinction coefficient sensor of a runway visual range system. These issues were addressed in Chapters 3, 5 and 6.

2. An extensive test program showed that the national deployment version of the new generation forward scattermeter performs well under all common meteorological conditions. The continuing work described in Chapter 7 will extend this evaluation to rare meteorological conditions.

3. The US forward scattermeter has been demonstrated to meet the needs of an automated RVR system for use with precision runways under all weather conditions.

APPENDIX A - OTIS REPRESENTATIVENESS METHODOLOGY

A representativeness analysis has the opposite requirements from the scattermeter calibration analysis presented in Section 5.2:

1. The calibration analysis seeks to isolate conditions when two instruments will agree unless they have inherent differences. The forward scattermeters are located near the crossing point of the perpendicular transmissometers in order to obtain the best correlation between the test and reference sensors. Homogeneity criteria are then applied (Section 5.2.3) to further improve the correlation between the sensors.

2. The representativeness analysis looks for conditions where two identical instruments at different locations may disagree. Therefore, no homogeneity criterion is applied. As shown in Figure 22, the Otis site permits a comparison between two 152-meter-baseline transmissometers that are displaced by 152 meters, which is just the displacement of a US extinction coefficient sensor from the runway centerline. The measurement of a "virtual" displaced transmissometer T5 can be derived* from the measurements of the 152- and 304-meter transmissometers (T1 and T4) which use a common projector: $\sigma_4 = (\sigma_1+\sigma_5)/2$. The resulting σ_5 value for the displaced transmissometer is labeled "T000" in the following data plots.

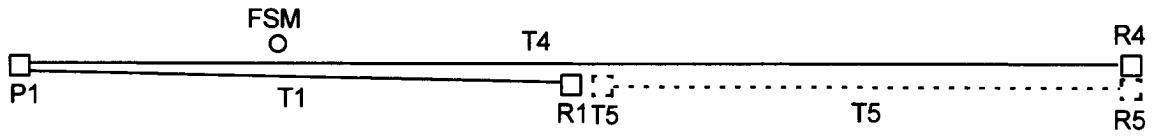

Figure 22. Virtual Displaced Transmissometer at Otis Weather Test Facility

Since no homogeneity criteria are applied in a representativeness study, the results are sensitive to transmissometer performance problems that may have been eliminated by the homogeneity criteria. All three transmissometers (T300, T500, and T000) must be operating properly for the analysis to be valid. The first attempt at this analysis used the first golden sensor test period presented in Section 5.3.2. Because of the frequent effects of snow on transmissometer performance, this period proved to be unworkable. The first analysis presented below, therefore, used an earlier summer test period (April through October 1995); several days in July had to be eliminated to remove data points where one of the transmissometers was not operating correctly. The second golden sensor test period also proved to give a valid analysis. Both are presented below.

The analysis used the box plot method described in Section 5.2.5.1. The representativeness of the sensor measurements was quantified by the width of the FOG box (Figure 15) in the box plot comparing the sensor to the reference transmissometer. Because the 304-meter T4 transmissometer can measure only half the maximum extinction coefficient of a 152-meter transmissometer, the lower MOR range limit in Figure 16 had to be increased to log(MOR) = 2.3 to eliminate erroneous data.

---

* First, the σ_4 value from T4 is corrected by a factor of 0.963 to give a σ_4 value for visible light. Second, half the σ_1 value is subtracted and the result multiplied by a factor of two to give σ_5.

The results of the analysis are shown in Figures 23 and 24. The width of the box plot was calculated as the spread between the 75th and 25th percentile ratios normalized to the 50th percentile ratio. Three reference transmissometers and five or six sensors (two transmissometers and three or four scattermeters) are shown. Note that the position of a transmissometer is taken as the midpoint of its baseline. When the displacement between the sensor and reference is zero, the box width for transmissometers is roughly half that observed for the forward scattermeters. Note that, only the relationship between the crossed transmissometers (T300 versus T500) is relevant; each transmissometer, of course, agrees perfectly with itself. When the displacement between the sensor and reference transmissometer is increased to 152 meters, however, the box spread increases for both types of sensors and becomes comparable. Since this displacement corresponds to the minimum US separation between the extinction coefficient sensor and the strip of runway it is required to represent, one must conclude that there is no significant difference in the operational representativeness of the transmissometer and the forward scattermeter.

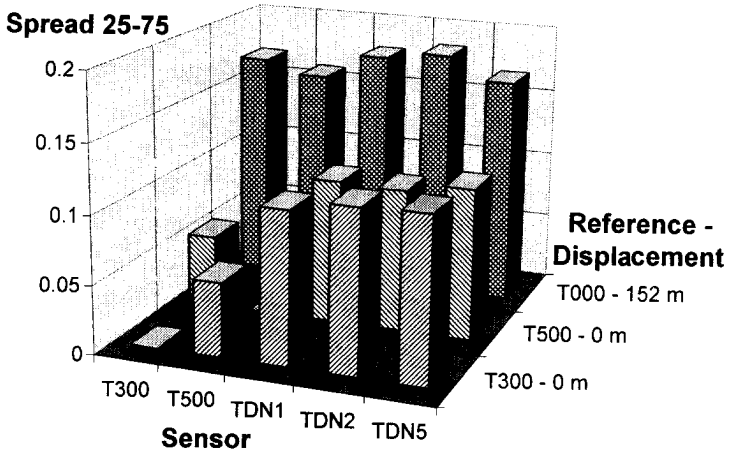

Figure 23. Box Width as a Function of Reference Transmissometer Displacement for Transmissometers T300 and T500 and Forward Scattermeters TDN1,2,5 (4/1/95-10/31/95)

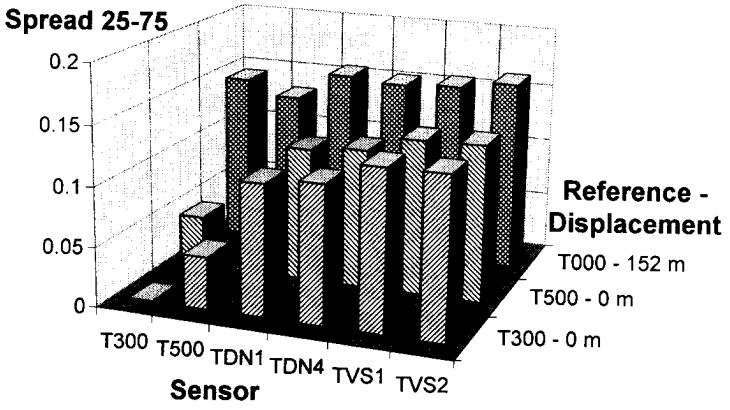

Figure 24. Observed Box Width as a Function of Reference Transmissometer Displacement for Transmissometers T300 and T500 and Forward Scattermeters TDN1,4 TVS1,2-3 (4/29/96-8/12/96)

APPENDIX B - FIELD TEST DATA PROCESSING

The processing of the Otis WTF data consists of the following steps:

1. Create binary performance files of one-minute averages for each sensor from the daily raw data files. The last engineering data port (EDP) report of the minute was used for the new generation RVR sensors.

2. Combine the performance files for the entire test period into a single file. For example, the file for the first golden test period was called GOLD1 (39 Mbytes).

3. Correct the 100-percent readings of the reference transmissometers by comparisons with an HSS forward scattermeter (termed HSB1) whenever the visibility is above 30 km. The corrected file name for the first golden test period became GOLD1.CTH.

4. Evaluate sensor calibration using the box-plot method (see Section 5.2.3.2).

5. Require homogeneous conditions by comparing the two crossed visible-light reference transmissometers, termed T300 and T500, with baselines respectively of 91 and 152 meters (300 and 500 feet). Include data when the difference in σ value measured by the two transmissometers is less than a specified percentage of their average value.

6. Use an HSS present weather sensor (termed PW67) to estimate precipitation rate (parameter PR67) to distinguish conditions of precipitation and no precipitation, and precipitation type (parameter WX67) to distinguish rain and snow. When the temperature is above 42° F, any snow reports are changed to rain.

REFERENCES

[1] Thomas, D.C., "Assessment of Runway Visual Range on Runways," *Journal of Science & Technology*, Vol. 37, No. 2, 1970, pp. 65-73.

[2] West, M., and Burnham, D., "Analysis of Runway Visual Range Errors," "First Symposium on Integrated Observing Systems," 2-7 February 1997, paper J10.7.

[3] Middletom, W.E.N., *Vision Through the Atmosphere*, University of Toronto, 1952.

[4] Burnham, D.C., "Evaluation of Visibility Sensors at the Eglin Air Force Base Climatic Chamber," Report No. DOT/FAA/PM-83/29, October 1982.

[5] Griggs, D.W., Jones, D.W., Ouldridge, M. and Sparks, W.R., "The First WMO Intercomparison of Visibility Measurements, Final Report," WMO/TD No. 401, 1990.

[6] Muench, H.S., Moroz, E.Y., and Jacobs, L.P., "Development and Calibration of the Forward Scatter Visibility Meter." Report No. AFCRL-TR-74-0145, Air Force Cambridge Laboratories, March 1974.

[7] Burnham, D.C., "High Visibility Measurements and Reference Standards," Seventh Symposium on Meteorological Observations and Instrumentation, Jan. 14-18, 1991, pp. 332-337.

[8] West, M.D., Burnham, D.C., and Miles, C.S., "Snow Performance of the New Generation Runway Visual Range (RVR) System," Sixth Conference on Aviation Weather Systems, 15-20 January 1995, pp. 357-361.

[9] West, M., Crovo, J. and Burnham, D., "Laboratory Simulation of Blowing Snow Effects on Optical Sensors of RVR System," "First Symposium on Integrated Observing Systems," 2-7 February 1997, paper J10.10.

[10] Schwartz, D and Burnham, D. "Otis ANGB Visibility Sensor Field Test Study," Report No. AFGL-TR-86-0011(I), Feburary 1987; Appendices in Report No. AFGL-TR-86-0011(II).

[11] Department of Transportation, Federal Aviation Administration Specification: Runway Visual Range System, FAA-E-2772, October 30, 1985.

[12] West, M.D., Burnham, D.C., and Miles, C.S., "Validation of the New Generation Runway Visual Range (RVR) System for Category IIIb," Sixth Conference on Aviation Weather Systems, 15-20 January 1995, pp. 351-356.

[13] Pawlak, R. and Burnham, D., "Accuracy Validation of the Scattermeter for the FAA New Generation Runway Visual Range System," "First Symposium on Integrated Observing Systems," 2-7 February 1997, paper J10.8.

[14] West, M.D., Burnham, D.C., and Miles, C.S., "Calibration Error Simulation for Forward Scatter Visibility Sensors," Sixth Conference on Aviation Weather Systems, 15-20 January, 1995, pp. 341-346.

[15] Burnham, D.C. and Phillips, C.O., "Validation of a Forward-Scatter Visibility Sensor for RVR Measurements," World Meteorological Organization, Instruments and Observing Methods, Report No. 49, WMO Technical Conference on Instruments and Methods of Observation, 11-15 May 1992, pp. 320-324.

[16] Burnham, D.C., "Fog, Snow and Rain Calibrations for Forward-Scatter Visibility Sensors," Eighth Symposium on Meteorological Observations and Instrumentation, 17-22 January 1993, pp 66-71.

[17] Burnham, D.C., "Rain Response of Forward-Scatter Visibility Sensors," Fifth Symposium on Meteorological Observations and Instrumentation, 11-15 April 1983, pp. 102-104.

[18] D'Errico, R.E., Hazen, D.A., Burnham, D.C., and Miles, C.S., "Application of Frequency of Occurrence Data Derived from Surface Aviation Observations in the Evaluation of Visibility Sensor Performance," Ninth Conference on Applied Climatology, 15-20 Jan 1995, pp. 7-12.

☆U.S. GOVERNMENT PRINTING OFFICE: 1997 - 501-031